UNIVERSITÀ
DEGLI STUDI
DI PADOVA

Sede Amministrativa: Università degli Studi di Padova

Dipartimento di Medicina Animale, Produzioni e Salute

CORSO DI DOTTORATO DI RICERCA IN: Scienze Veterinarie

CICLO XXX

TOMOGRAPHIC IMAGING IN COMPANION AVIAN SPECIES

Coordinatore: Ch.mo Prof. Alessandro Zotti

Supervisore: Ch.mo Prof. Alessandro Zotti

Dottorando: Irene Alessandra Veladiano

Index

Abstract

Background

In the last decades an increasing number of publications, proposing both clinical trials and diagnostic tests, have become available on avian medicine. Despite all the new technical advances the diagnosis and treatment of avian patients is still challenging for the veterinary clinician because birds often display only vague and non-specific symptoms of disease and the investigation of the underlying causes is often very frustrating. In such a scenario diagnostic imaging plays a fundamental role in the clinical evaluation of avian patients.

Results

The result of this PhD research is an atlas of the tomographic anatomy of three avian species. Most of the clinically relevant structures of the head were visible in both the cross-sections and corresponding CT images. The thin trabeculae characterizing the avian skull were optimally visible on CT images when a standard soft tissue filter and pulmonary window was used. The same CT settings allowed clear visualization of the nostrils, operculum, infraorbital sinus, and cervicocephalic air sacs. The nasal septum, conchae, scleral ossicles, interorbital septum, auditory meatus, and hyoid skeleton were clearly identifiable when a high-resolution filter and bone window were used. Reconstruction of CT images in a dorsal plane enabled a more comprehensive visual examination of some complex structures of the head, such as the diverticula of the infraorbital sinus and the periorbital muscles and glands.

Structures of the inner ear were not visible in the anatomic cross-sections nor in the CT scans of any of the examined parrot species.

A standard soft tissue filter with a soft tissue window allowed a good visibility of the eyes and related structures in all examined species. The cerebral hemispheres, cerebellum, and medulla oblongata were distinguishable only on anatomic cross-sections, and all had the same soft tissue attenuation.

All the main organs of the respiratory, digestive, urinary (including the ureters) and reproductive systems were visible both in the anatomical sections and in the corresponding CT images.

Conclusions

CT is a fast, safe and reliable diagnostic test for avian patients. The possibility to scan the entire body, avoiding the superimposition of the radiography is a great improvement in the diagnostic process. Furthermore, the use of contrast medium allowed optimal visibility of the soft tissues.

Those findings suggested that the complex nature of the avian anatomy make CT the diagnostic imaging technique of choice for the evaluation of both the coelomic cavity and the head of avian patients.

The matched anatomical cross-sections and CT images presented in this study are a useful reference for the interpretation of CT examination of the blue-and-gold macaw, African grey parrot and monk parakeet. This atlas can be used also for the interpretation of CT images obtained in other psittacine species but the clinicians should be aware of the anatomical differences occurring between the species investigated in these studies and the species object of the investigation. For this reason, further studies, including a larger number of both

psittacine and non-psittacine species are desirable for a more comprehensive description of the CT anatomy of avian patients.

Introduction

Men have observed birds from the ancient times; the first evidence of this interest is a petroglyph of the Paleolithic age, discovered in Cadice (Spain)[1]. Proceeding through the history of mankind it is possible to find several examples of the bond between these animals and humans.

The first written evidence of accurate and "scientific" descriptions and observations of birds was found with the Veda population back in 1500 a.C. [2]. Also figurative art of the ancient populations of China, Japan and India testify a great interest for birds[3].

"Parrot" is a generic term that refers to animals belonging to the order *Psittaciformes*. This order counts approximately 383 species, divided into four families[4]. The majority of those species are endemic of the tropical and subtropical regions of the world, but, animals belonging to the order *Psitacciformes* can be found as pet at any latitude. It some cases colonies of parrots can be also found in cities (for example Rome) located far away from the usual habitat of these animals; most likely these colonies originated from escaped pet animals that survived and flourished in the urban environment.

In the whole bird clade, parrot birds stand out for their beautiful color, the ability to reproduce sounds, their great intelligence and their complex social behavior. The possibility to create a tight relationship with those animals are the reasons that have encouraged people to tame and breed different species of parrots. The ability to interact with humans and the long-life expectancy allow them to become part of the family. It is not uncommon to find a pet parrot older than the owner, that inherit the animal from his parents.

The sentimental bond is one of the main reason that lead the owner of those animal to ask for very specific medical treatment for their pet.

References

1. Gurney JH. Prehistoric birds. In: Gurney JH, editor. Early Ann. Ornithol. 1st ed. High Holborn, London: H.F. & G. Witherby; 1921. p. 1–13.

2. Ali S. Bird study in India: its history and importance. In: ICCR, editor. Azad Meml. Lect. New Dheli: ICCR; 1979.

3. David L. Enjoying ornithology. London, UK: Methuen & Co. Ltd; 1965.

4. Parrots & cockatoos « IOC World Bird List [Internet]. [cited 2017 Jul 26]. Available from: http://www.worldbirdnames.org/bow/parrots/

Chapter I: Avian medicine

Avian medicine has faced a marked improvement in the last decades. Even if the number of pet birds was stable in the last years[1] the owners' attention and concern about their pets are constantly growing and therefore the request for high quality veterinary care is also increased.

At the same time, the number of veterinarians specialized in avian medicine is significantly[2] increased. In the last two decades there was an increased research activity in the avian medicine field and several publications investigating behavioural problems[3,4], infectious and parasitic disease[5-9], assessment of the specie-specific blood reference values[10] and artificial reproduction[11,12] became available.

Such improvement is also assisted by several new diagnostic tests available for avian patients, thanks to the combination of increasing interest and refinement of the medical technologies. For example, new diagnostic instruments allowing to perform a complete blood work with small amounts of blood, along with the increased number of hematological parameters available for avian species have lead an increase knowledge in the avian internal medicine field.

Despite the recent technical innovations avian medicine still challenging and can be, sometimes, very frustrating, because birds are so-called stoic animals and hide almost every sign of illness.

It is not uncommon to investigate birds with vague and non-specific symptoms caused by severe underlying pathologies. In such a scenario diagnostic imaging is a very important diagnostic tool.

Radiographic examination is a quick and inexpensive diagnostic tool and, most of the times, can be performed with unsedated animals and it allows to detect obvious pathologic changes. The bidimensional nature of radiographic images, leading to the superimpositions of several structures, along with the limited spatial resolution act as limiting factors in the detection of pathological changes, especially of the respiratory apparatus. In this region the lesions detected by the mean of the radiography are the 40% of the total lesions detected with the CT scan[13].

Ultrasnographic investigation is feasible in avian patients, but the presence of the feathers and the air sacs limit the number of available acoustic windows thus making this examination challenging. In most patients is impossible to thoroughly evaluate all the coelomic structure and therefore to achieve a correct diagnosis. Nevertheless, in selected cases (for example when abnormal fluid-filled structures are found near the coelomic wall) ultrasound is reported to be useful for a quick evaluation of the coelomic cavity in avian species[14].

CT examination allows to perform whole-body scans in a limited amount of time. Moreover, the three dimensional nature of CT images avoids superimpositions thus allowing a thorough investigation of all the stuctures of the coelomic cavity. The use of contrast medium allows to detect lesions that are otherwise impossible to identify with other diagnostic techniques. Even if the spatial resolution is still a limiting factor when imaging

small-sized animals, with the modern CT-scan is possible to obtain acceptable images of animals of 80 grams[15,16].

Moreover, the possibility to use different reconstruction algorithms, and to visualize the images with different windows to selectively investigate bones, lungs, and soft tissues, increases the chance to correctly identify pathological changes of the coelomic organs.

References

1. ASSALCO. Rapporto ASSALCO-ZOOMARK 2015 Alimentazione e cura degli animali da compagnia. 2015.

2. ECZM. Avian Specialty [Internet]. [cited 2017 Aug 17]. Available from: https://www.eczm.eu/Avian Specialty.asp

3. Schwing R, Nelson XJ, Wein A, Parsons S. Positive emotional contagion in a New Zealand parrot. Curr. Biol. 2017;27:R213–4.

4. de Souza Matos SL, Palme R, Vasconcellos SA. Behavioural and hormonal effects of member replacement in captive groups of blue-fronted amazon parrots (*Amazona aestiva*). Behav. Processes. 2017;138:160–9.

5. Razmyar J, Rajabioun M, Zaeemi M, Afshari A. Molecular identification and successful treatment of Chlamydophila psittaci (genotype B) in a clinically affected Congo African grey parrot (*Psittacus erithacus erithacus*). Iran. J. Vet. Res. 2016;17:281–5.

6. Högemann C, Richter R, Korbel R, Rinder M. Plasma protein, haematologic and blood chemistry changes in African grey parrots (*Psittacus erithacus*) experimentally infected with bornavirus. Avian Pathol. 2017;1–15.

7. Vaz FF, Serafini PP, Locatelli-Dittrich R, Meurer R, Durigon EL, de Araújo J, et al. Survey of pathogens in threatened wild red-tailed Amazon parrot (*Amazona brasiliensis*) nestlings in Rasa Island, Brazil. Brazilian J. Microbiol. 2017;48(4):747-753.

8. Rubbenstroth D, Schmidt V, Rinder M, Legler M, Twietmeyer S, Schwemmer P, et al. Phylogenetic Analysis Supports Horizontal Transmission as a Driving Force of the Spread of Avian Bornaviruses. Lierz M, editor. PLoS One. 2016;11:e0160936.

9. Huang Y-L, Tsai S-S, Thongchan D, Khatri-Chhetri R, Wu H-Y. Filarial nematode infection in eclectus parrots (*Eclectus roratus*) in Taiwan. Avian Pathol. 2017;46:188–94.

10. Vaz FF, Locatelli-Dittrich R, Beltrame OC, Sipinski EAB, Abbud MC, Sezerban RM. Hematologic and biochemical reference intervals of free-living Red-Tailed Amazon parrot (*Amazona brasiliensis*) nestlings on Rasa Island, Paraná, Brazil. Vet. Clin. Pathol. 2016;45:615–22.

11. Scagnelli AM, Tully TN. Reproductive Disorders in Parrots. Vet. Clin. North Am. Exot. Anim. Pract. 2017;20:485–507.

12. Bublat A, Fischer D, Bruslund S, Schneider H, Meinecke-Tillmann S, Wehrend A, et al. Seasonal and genera-specific variations in semen availability and semen characteristics in large parrots. Theriogenology. 2017;91:82–9.

13. Huynh M, Modesto F, Zoller G, Chassang L. Use of conscious whole body dorsoventral radiograph in psittacine presented for respiratory distress:comparison of in-box radiograph, standard radiograph and computed tomodensitometry. In: Azmanis P, Chitty J, Crosta L, Huynh M, Lierz M, Montesinos Barcelò A, et al., editors. 3rd Int. Conf. avian Herpetol. Exot. mammal Med. Abbiategrasso (MI): Press Point srl; 2017. p. 831.

14. Krautwald-Junghans M-E, Pees M. Ultresonographic examinations. In: Krautwald-Jughanns ME, Pees M, Reese S, Tully T, editors. Diagnostic imaging Exot. pets. Hannover: Schlütersche Verlagsgesellschaft mbH & Co. KG; 2011. p. 36–53.

15. Veladiano IA, Banzato T, Bellini L, Montani A, Catania S, Zotti A. Computed tomographic anatomy of the heads of blue-and-gold macaws (*Ara ararauna*), African grey parrots (*Psittacus erithacus*), and monk parakeets (*Myiopsitta monachus*). AJVR 2016, 12:77.

16. Veladiano IA, Banzato T, Bellini L, Montani A, Catania S, Zotti A. Normal computed tomographic features and reference values for the coelomic cavity in pet parrots. BMC veterinary research 2016, 12:182.

Chapter II: Scientific aim of the thesis

The objective of my research activity was the standardization of some diagnostic imaging techniques, mainly computed tomography, on avian patients.

In particular the focus was to create an atlas of the computed tomographic anatomy of parrots.
It was impossible to include all the species belonging to the order of *Psitacciformes*, and therefore the three of the most common pet parrot species (*Ara ararauna*, *Psittacus erittacus* and *Myopsitta monachus*) were choose for this research.

The use of computed tomography in avian patients was already reported at the time of these studies, but no complete reference of the normal tomographic anatomy of the parrots was available.

Even if nowadays the use of CT is widespread in veterinary medicine, the lack of a reliable reference on the normal tomographic anatomy of parrots is, most likely, one of the main reason that prevent a lot of veterinary practitioner to suggest a CT scan examination in avian patients.

The creation of an atlas of the normal tomographic anatomy of avian species is the first step to promote the diffusion of this diagnostic technique in parrot patients. Moreover, the possibility to obtain high quality images even in small birds should further increase the diffusion of this diagnostic technique in avian medicine.

Despite the presence of interspecific and even intraspecific anatomic differences in parrots' anatomy this work represents the first step to fill the existing gap.

Hopefully this will be the first of numerous papers that will lead to a widened knowledge of the tomographic anatomy of those species.

Chapter III: Anatomic peculiarity of the parrot

Parrot anatomy is characterized by unique features, developed in response to the necessity of the flight and of their peculiar seed-based diet.

A thorough knowledge of avian anatomy is mandatory both for clinical examination and diagnostic imaging procedures.

Skeletal system

Parrots' skull is almost spherical, composed by numerous pneumatized bones, that can be divided in 7 portions: occipital complex, sphenoid complex, squamosal, otic complex, parietal, frontals, ethmoid complex, prefrontal.

Usually in the adult bird is almost impossible to distinguish the suture between the bones; this characteristic adds strength to the birds' skull [1–3].

The upper and the lower jaws are covered by a keratinized layer that forms the rhamphotheca, that can be further divided in the rhinotheca and the gnatotheca [2].

The total number of vertebrae composing the vertebral column varies among parrot species. Both intra- and inter-specific variability is reported. As a rule of thumb most parrot species have thirty-six vertebrae divided as follows: 12 cervical, 8 thoracic, 8 lumbosacral and 8 caudal. The number of vertebrae composing the cervical colum is reported to have the larger variability [3]. Most of the thoracic, lumbosacral and caudal vertebrae are fused and therefore individual vertebrae are often difficult to identify. The diverticula of the air sacs penetrate into the vertebral column making these latter pneumatized bones. Specifically, the cervical and cranial thoracic vertebrae are in communication with the cervical air sacs and the caudal thoracic vertebrae and synsacral vertebrae with the abdominal air sacs [4].

Respiratory system

The nares are located in the dorsal portion of the rhinoteca. Each nasal cavity is divided into two halves by a septum. Each nasal cavity is further divided into a rostral, a medium and a caudal nasal concha in most parrot species. Inside each nostril a corneus flap of tissue, called operculum, protrudes.

The pharynx is the common chamber of the mouth and the nasal cavity that includes the opening of both the esophagus and the glottis. The dorsal roof of the pharynx is formed by the palatine folds, that extend from the inner margin of each side of the upper jaw in direction of the midline, between the folds remain a slit, the so-called choana [3].

The caudal nasal concha opens dorsally in the infraorbital sinus, and has no connections with the nostrils [5].

The infraorbital sinus is located lateral to the nose and surround the eyes ventrally. It is divided into five diverticula and extends into the upper beak, mandible and portion of the pneumatic skull. Caudally the sinus opens in the cervicocephalic air sac. The infraorbital sinus is the only sinus in birds and his lateral wall is made only by skin and subcutaneous tissue [5].

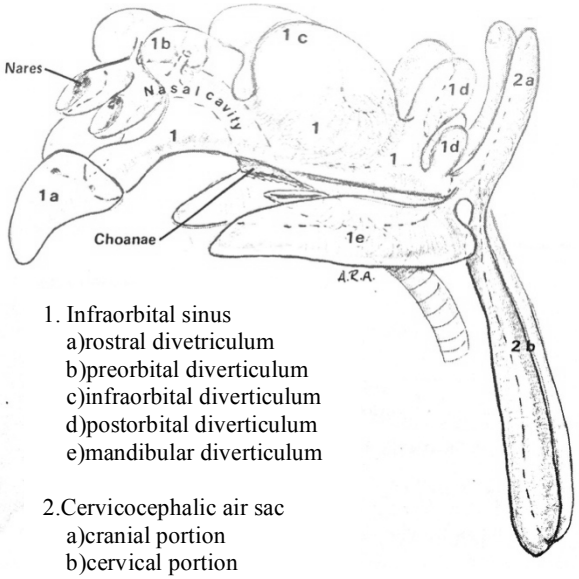

1. Infraorbital sinus
   a)rostral divetriculum
   b)preorbital diverticulum
   c)infraorbital diverticulum
   d)postorbital diverticulum
   e)mandibular diverticulum

2.Cervicocephalic air sac
   a)cranial portion
   b)cervical portion

Image from: Hasrrison GJ, Harrison LR editors. Clinical avian medicina and surgery, including aviculture. Philadelphia: WB Saunders company; 1986. P. 47

The trachea is composed by complete cartilaginous rings, that occasionally are calcified [2].

At the end of the trachea is located the syrinx, the birds' vocal organ.

This structure is composed of modified cartilaginous structures and associated membranes and muscles.

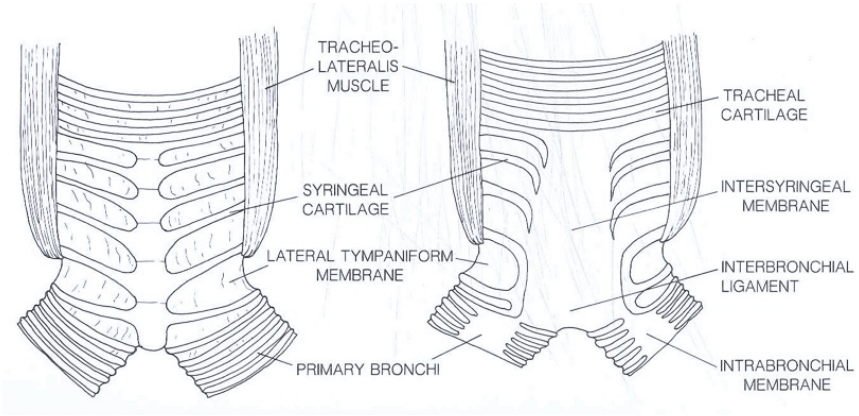

Ventral (left) and dorsal (right) views of the syrinx

Image from: Chiasson RB, editors. Laboratory anatomy of the pigeon Third ed. Dubuque, Iowa: Wm. C. Brown Publishers; 1959. p. 58

The trachea splits into two main stem bronchi that have both an extra and an intra pulmonary portion. The main stem bronchi enter the craniomedial surface of the lungs and then run caudolaterally. The wall of the bronchi is composed by C shaped cartilaginous rings closed on the medial surface by a thin and elastic tissue [2]. Arborization starts in the intrapulmonary portion of the main stem bronchi with secondary and tertiary bronchi, named also parabronchi [2].

The lungs are located cranio-dorsally in the coelomic cavity and extend between the first and the seventh rib. Parrots' lungs have a minimal expansion capability and are strictly attached to the ribs, filling the intercostal spaces. The avian respiratory system is characterized by the presence of nine air sacs; the paired

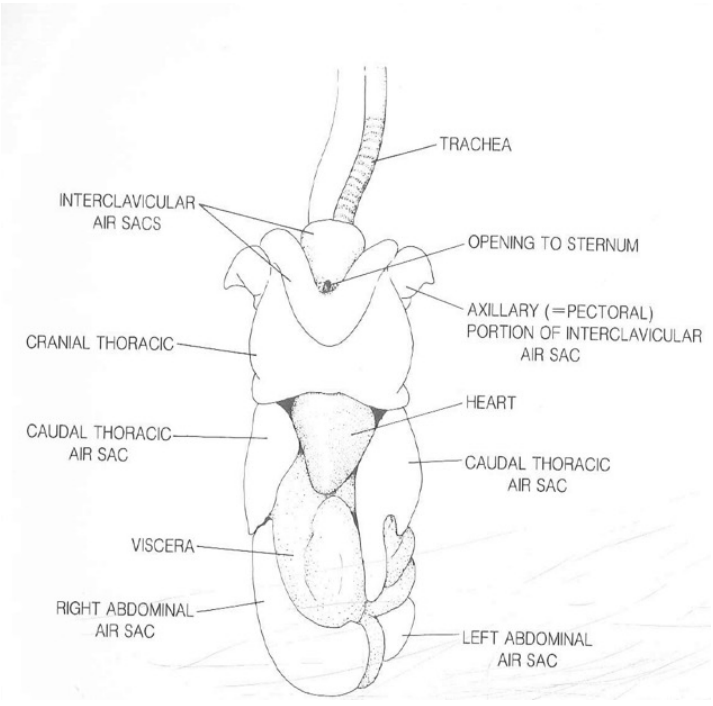

Ventral view of the air sacs

Image from: Chiasson RB, editors. Laboratory anatomy of the pigeon Third ed. Dubuque, Iowa: Wm. C. Brown Publishers; 1959. p. 59

cranial thoracic, caudal thoracic and abdominal air sacs and the unpaired clavicular air sac, that lies caudal to the crop in the thoracic inlet [5].

Circulatory system

Birds' heart is a four-chambered structure, located in the cranio-ventral portion of the coelomic cavity with the apex located in a caudo-medial position. The avian heart is characterized by the presence of the *sinus venosus,* a partially separated chamber located at the confluence of the cranial and caudal vena cava, that opens in the right atrium. The aorta emerges from the left ventricle; after a few centimetres forms the right aortic arch and extends caudally[6].

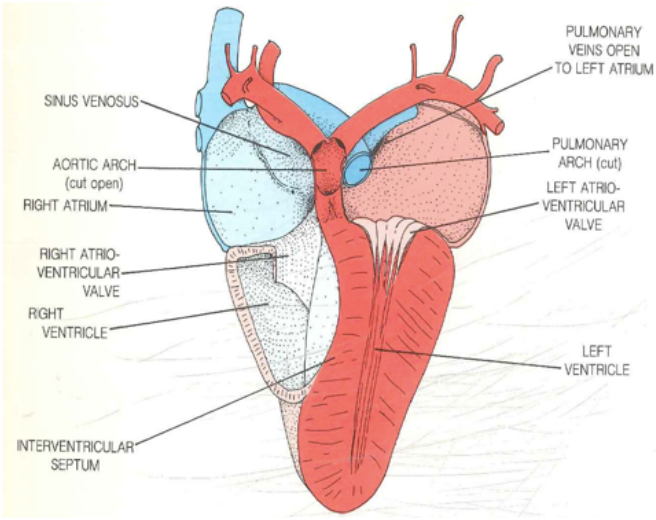

Ventral view of the pigeon heart sectioned in the dorsal plane.

Image from: Chiasson RB, editors. Laboratory anatomy of the pigeon Third ed. Dubuque, Iowa: Wm. C. Brown Publishers; 1959. p. 65

The pulmonary arch emerges from the right ventricle. This structure divides into right and left pulmonary arteries dorsal to the bifurcation of the aortic arch.

All the veins of the avian heart drains into the cranial vena cava, caudal vena cava or in the hepatic portal veins.

Each cranial vena cava is formed by the convergence of subclavian veins, jugular veins and pectoral trunk; the caudal vena cava originates from the union of the two common iliac veins, than passes through the liver, where it receives the hepatic veins and emerges from the liver to enter the dorsal surface of the sinus venosus [1].

Birds' oral cavity is an undivided space containing the oral and pharyngeal cavity. Parrots' tongue is a mobile, protrusible blunt structure, with a cylindrical shape. It is characterized by the presence of intrinsic musculature and usually does not have taste buds[1,7]. The mobility is different in relation to the parrot specie.

The tongue and the associated muscles are supported by the hyobranchial apparatus; those structures form a large portion of the floor of the pharynx.

The glottis is a raised area located on the centre of the laryngeal prominence. This structure is visible on the floor of the pharynx, between the tongue and the esophagus.

The avian stomach is composed by two distinct portions, the proventriculus and the ventriculus (also called gizzard) connected by an intermediate zone, called isthmus.

The proventriculus is the glandular portion of the stomach and is located caudal to the liver occupying the left dorsal and ventral region of the coelomic cavity.

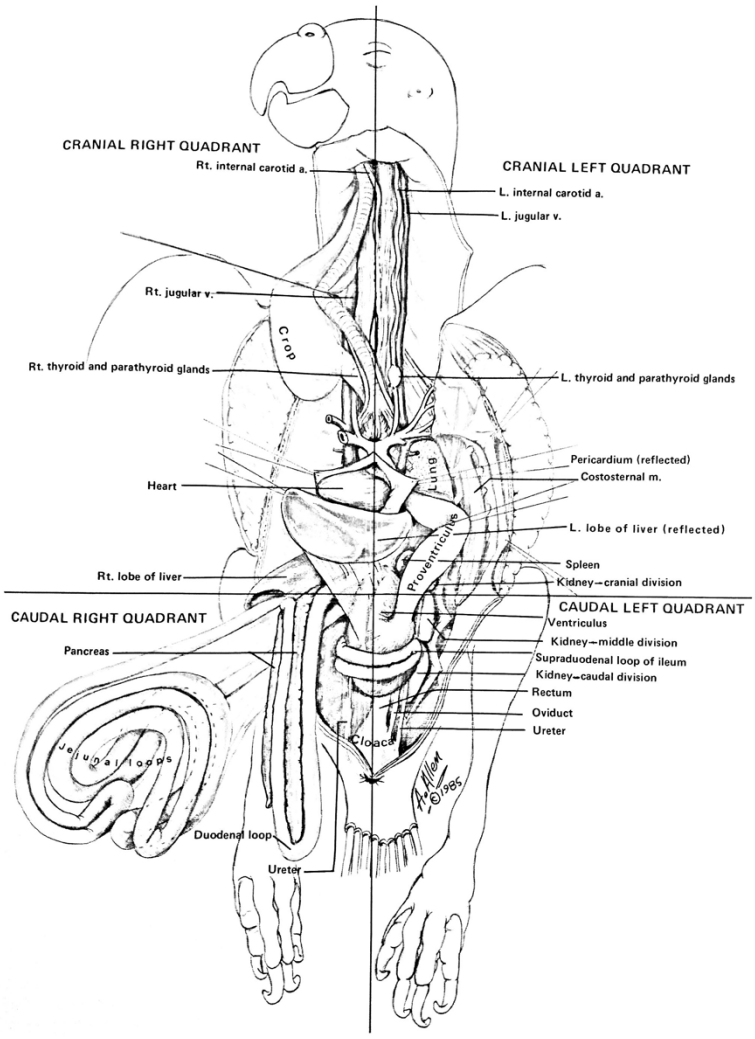

Internal structures and quadrants of the Amazon Parrot (deep ventrodorsal view with reflection of viscera).

Image from: Hasrrison GJ, Harrison LR editors. Clinical avian medicina and surgery, including aviculture. Philadelphia: WB Saunders company; 1986. P. 55

The ventriculs is the muscular part of the stomach. It is located immediately caudal to the proventriculus. This organ is assigned to the mechanic digestion and has a thick wall composed by smooth muscles.

The duodenum is a narrow U-shaped organ starting at the junction between ventriculus and proventriculus; in this way, the food that doesn't need additional mechanical digestion can move directly into the intestine. The pancreas is located inside the duodenal loop[2]. The small intestine is the longer portion of the intestine and it is composed by three primary loops called duodenal, umbilical, and supraduodenal.

The large intestine is short and straight with the caecum marking the distinction between the small and the large intestine. The rectum begins near the gizzard and runs parallel to the vertebral column into the cloaca.

The cloaca is the terminal part of both the digestive and the urinary system. The rectum enters in the mid-ventral part of the cloaca called coprodeum. Both coprodeum and urodeum open in a common chamber, the proctodeum, connected outside to the vent [2].

The liver is a bilobed structure, with the right lobe being larger than the left in most parrot species, located in a cranio-ventral position, just above the sternum.

Parrots lack gallbladder in most of the species and both the left and the right hepatic ducts drain directly into the duodenum [8].

The spleen is a rounded organ located in the median portion of the coelomic cavity, on the right side of the proventriculus, in between the ventriculus and the proventriculus[9].

The pancreas is located in the ventral portion of the coelomic cavity, slightly on the left, between the loops of the descending and ascending duodenum, and is embedded within the mesoduodenal ligament[6,7].

Avian kidneys are two paired structures located in the dorso-caudal portion of the coelomic cavity, inside a depression of the pelvis. Each kidney has a cranial, a middle, and a caudal lobe. Histologically the transition between the cortex and the medulla is indefinite. Three individual renal arteries supply blood to each renal lobe. Parrots also have a renal portal system with the renal portal veins carrying blood to the glomeruli in addition to the renal arteries. Blood from the large intestine, pelvic region and legs is drained to the kidneys by the caudomesenteric, pelvic and ischiatic veins[2].

Each kidney has a ureter originating from the ventral portion of the cranial lobe and running caudally on the ventral surface of the middle and caudal lobe. The ureters run caudally and enter dorsally into the urodeum, the do rsal part of the cloaca[10].

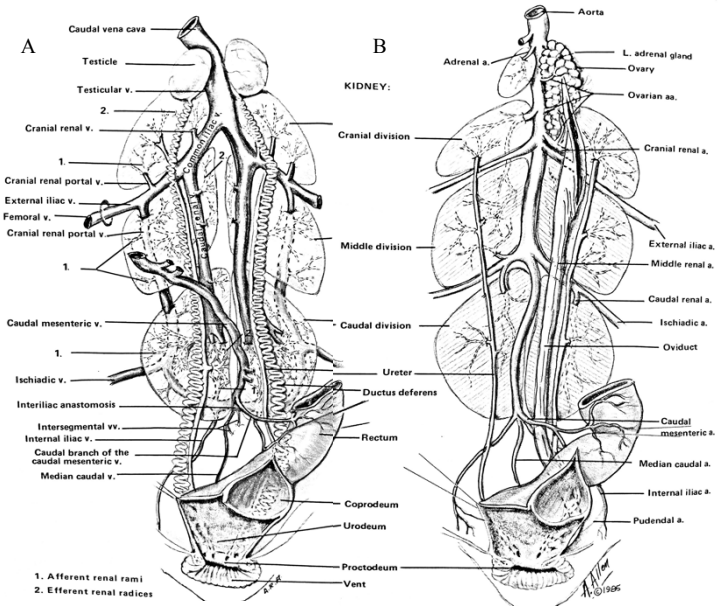

Urogenital system of the amazon parrot. A: male B: female

Image from: Hasrrison GJ, Harrison LR editors. Clinical avian medicina and surgery, including aviculture. Philadelphia: WB Saunders company; 1986. P. 58

Adrenal glands are paired organs located cranio-medially to the corresponding kidney[11].

In parrots the gonads are located inside the coelomic cavity. Males have paired testicles, located medio-ventrally to the cranial lobe of the kidneys. They are surrounded by the abdominal air sacs and the air passing through the air sacs is thought to be cooling the testes[6].

Females have only one fully developed ovary, in most species is the left one. The right ovary degenerates in early pre-natal life. During the reproductive season the testes can increase their dimensions up to 500 times. In the same way the ovary develops numerous follicles [12].

Nervous system

Avian brain is agyric, with no convolutions. As in mammals the brain is surrounded by three meninges: pia matter, arachnoid and dura mater, with the cerebrospinal fluid contained in the subarachnoideal space.

The olfactory bulbs are the most rostral part of the brain. The cerebral hemispheres are large, globous, structures located caudo-dorsal to the olfactory bulbs.

The optic lobes, located lateral to the optic chiasm are huge compared to the whole brain size, and are the major components of the midbrain.

The cerebellum is located in the caudal portion of the brain. It is composed by a single median lobe with the presence of a median sulci. The pons is poorly developed.

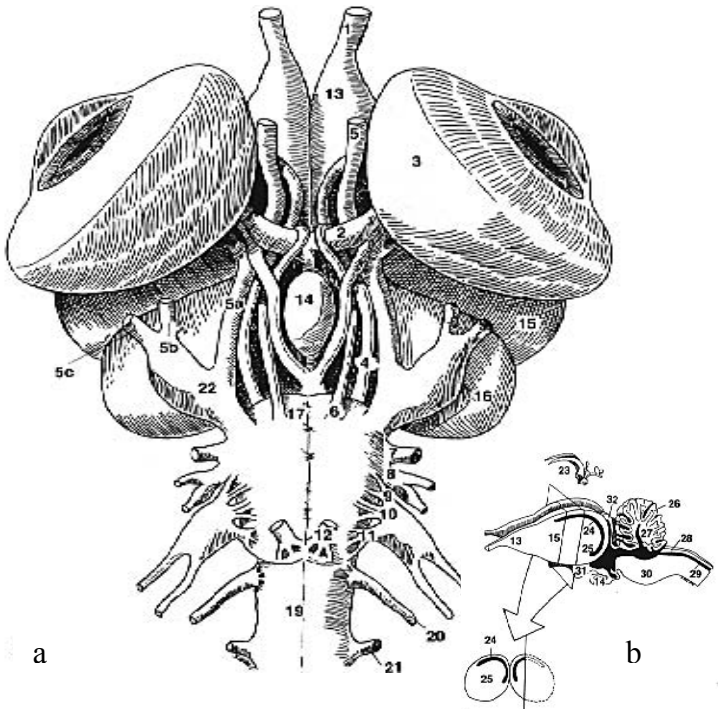

a) Ventral and b) lateral view of the brain. 1) cranial nerve I 2) cranial nerve II 3) eye 4) cranial nerve IV 5a) cranial nerve V (ophthalmic branch) 5b) cranial nerve V (maxillary branch) 5c) cranial nerve V (mandibular branch) 6) cranial nerve VI 7) cranial nerve VII 8) cranial nerve VIII 9) cranial nerve IX 10) cranial nerve X 11) cranial nerve XI 12) cranial nerve XII 13) olfactory lobe 14) pituitary gland 15) cerebral hemisphere 16) optic lobe 17) pons 18) medulla oblongata 19) spinal cord 20) cervical nerve 1 21) cervical nerve 2 22) trigeminal ganglion 23) ventricular system 24) lateral ventricle 25) corpus striatum 26) arbor vitae 27) cerebellum 28) roof of medulla oblongata 29) central canal 30) floor of medulla oblongata 31) optic chiasm and 32) pineal body.

Image from: Branson RW, Harrison GJ, Harrison LR, editors. Avian Med. Princ. Appl. 1st ed. Lake Worth, Florida: Wingers Publishing, Inc.; 1994. p. 525

Parrots have twelve cranial nerves: olfactory I, optic II, oculomotor III, trochlear IV, trigeminal V, abducens VI, facial VII, vestibulocochlear VIII, glossopharyngeal IX, vagus X, accessory XI, hypoglossal XII [1,3,13].

Eyes

Parrots' orbits are exceptionally large proportionately to the size of the skull. The main components of those structures are the orbitosphenoid, the frontals, the mesethmoid and the prefrontal bones. As for the majority of the skull, large part of this bones are pneumatized[14].

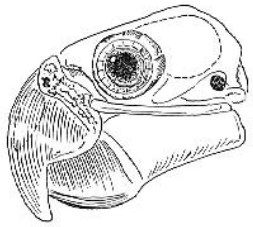

Relative size of the globe to the skull.
Image from: Branson RW, Harrison GJ, Harrison LR, editors. Avian Med. Princ. Appl. 1st ed. Lake Worth, Florida: Wingers Publishing, Inc.; 1994. p. 675

The orbital space lodges the eye, all the associated lacrimal glands, muscle vessels, nerves and a fat pad.

Depending on the species but also on interspecific variations the orbit may be close or open. When closed the orbit is completed rostroventrally by the suborbital arch[6].

Parrots' eyes are big globose structures, with the posterior segment bigger than the anterior.

As in mammals the globe is composed by three layers: sclera, chorioid and retina.

An osseous ring encircles the sclera; this structure, composed by numerous flat bones (11 to 15), avoid eyeball deformation due to the contraction of the ciliary muscles.

Differently from the mammals the muscular fibres of the ciliary body and of the pupil are striated.

Parrots have three eyelids; an upper and a lower one plus a nictitating membrane. The upper and the lower eyelids move vertically, whereas the nictitating membrane moves horizontally.

Within the orbit are located two glands: the lacrimal and the harderian gland[2,6]. A third gland, called nasal or salt gland is present in some birds such as budgerigars. It is located dorso-medial to the eye. This is a salt excreting and osmoregulatory gland.

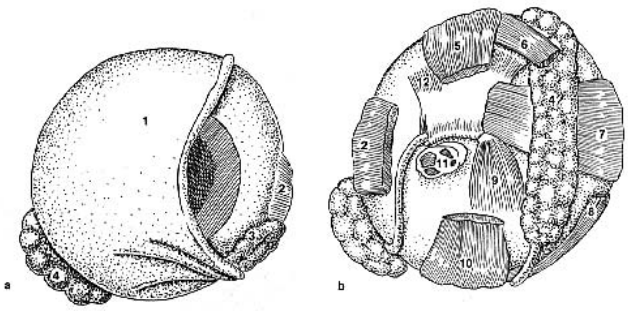

a) Anterior and b) Posterior view of the avian globe.
1) Nictitating membrane 2) M. lateral rectus 3) lacrimal gland 4) gland of nictitating membrane 5) M. dorsal rectus 6) M. dorsal oblique 7) M. medial rectus 8) M. ventral oblique 9) M. pyramidalis 10) M. ventral rectus 11) optic nerve and 12) M. quadratus (modified from Martin46).

Image from: Branson RW, Harrison GJ, Harrison LR, editors. Avian Med. Princ. Appl. 1st ed. Lake Worth, Florida: Wingers Publishing, Inc.; 1994. p. 676

Ears

Parrots' ears consist in an external, a middle and a short inner part. The external ear lacks the pinna and are covered by feathers. It is separated from the middle ear by the tympanum. Differently from the mammals the columella is the only bony ossicle of the middle ear [2,6].

References

1. Chiason RB. Laboratory anatomy of the pigeon. Lab. Anat. Ser. 1959. p. 54.

2. Evans HE. Anatomy of the budgerigar and other birds. S.l.: s.n.; 1996.

3. Harrison GJ, Harrison LR. Clinical avian medicine and surgery, including aviculture. 1st ed. Philadelphia: W.B. Saunders company; 1986.

4. Connor PMO. Pulmonary Pneumaticity in the Postcranial Skeleton of Extant Aves : A Case Study Examining Anseriformes. 2004;161:141–61.

5. Tulli TN, Harrison GJ. Pneumology. In: Ritchie BW, Harrison GJ, Harrison LR, editors. Avian Med. Princ. Appl. 1st ed. Lake Worth, Florida, Florida; 1994.

6. Chiasson RB. Laboratory anatomy of the pigeon. 3rd ed. Dubuque, Iowa: Wm. C. Brown; 1959.

7. Lumeij JT. Gastroenterology. In: Ritchie BW, Harrison GJ, Harrison LR, editors. Avian Med. Princ. Appl. 1st ed. Lake Worth, Florida: Wingers Publishing, Inc.; 1994. p. 482–514.

8. Lumeij JT. Hepatology. In: B. Ritchie, G. Harrison LH, editor. Avian Med. Princ. Appl. 1st ed. Lake Worth, Florida: Wingers Publishing, Inc.; 1994. p. 522–37.

9. Latimer, Kennet S., Rakich PM. Necropsy examination. In: Ritchie BW, Harrison GJ, Harrison LR, editors. Avian Med. Princ. Appl. 1st ed. Lake Worth, Florida: Wingers Publishing, Inc.; 1994. p. 355–81.

10. Lumeij JT. Nephrology. In: Branson RW, Harrison GJ, Harrison LR, editors. Avian Med. Princ. Appl. 1st ed. Lake Worth, Florida: Wingers Publishing, Inc.; 1994. p. 538–55.

11. Lumeij JT. Endocrinology. In: Branson RW, Harrison GJ, Harrison LR, editors. Avian Med. Princ. Appl. 1st ed. Lake Worth, Florida: Wingers Publishing, Inc.; 1994. p. 582–606.

12. Taylor M. Endoscopic examination and biopsy techniques. In: Branson RW, Harrison GJ, Harrison LR, editors. Avian Med. Princ. Appl. 1st ed. Lake Worth, Florida: Wingers Publishing, Inc.; 1994. p. 246–326.

13. Bennet RA. Neurology. In: Branson RW, Harrison GJ, Harrison LR, editors. Avian Med. Princ. Appl. 1st ed. Lake Worth, Florida: Wingers Publishing, Inc.; 1994. p. 723–747.

14. Machado M, Dos Santos Schmidt EM, Montiani-Ferreira F. Interspecies variation in orbital bone structure of psittaciform birds (with emphasis on Psittacidae). Vet. Ophthalmol. 2006;9:191–4.

Chapter IV: Computed tomographic anatomy of the heads of blue and gold macaws, African grey parrots and monk parakeets

This chapter is adapted from: Veladiano I.A., Banzato T., Bellini L., Montani A, Catania, Zotti A. Computed tomographic anatomy of the heads of blue and gold macaws, African grey parrots and monk parakeets. American Journal of Veterinary Research 2016;77:1346-1356

Abstract

The aim of this work is to create an atlas of the normal CT anatomy of the head of blue-and-gold macaws (*Ara ararauna*), African grey parrots (*Psittacus erithacus*), and monk parakeets (*Myiopsitta monachus*).

3 blue-and-gold macaws, 5 African grey parrots, and 6 monk parakeets and cadavers of 4 adult blue-and-gold macaws, 4 adult African grey parrots, and 7 monk parakeets were used for this work.

Contrast-enhanced CT imaging of the head of the live birds was performed with a 4-multidetector-row CT scanner. Cadaveric specimens were stored at –20^{o}C until completely frozen, and each head was then sliced at 5-mm intervals to create reference cross-sections. Frozen cross-sections were cleaned with water and photographed on both sides. Anatomic structures within each head were identified with the aid of the available literature, labeled

first on anatomic photographs, then matched to and labeled on corresponding CT images. The best CT reconstruction filter and window width and window level for obtaining diagnostic images of each structure was also identified.

Most of the clinically relevant structures of the head have been identified both in the cross-section and in the CT images. Optimal visualization of the bony structures was achieved with a standard soft tissue filter and pulmonary window. The use of contrast medium allowed a thorough evaluation of the soft tissues.

The labeled CT images and photographs of anatomic structures within the heads of common pet parrot species obtained in this study may be useful as an atlas to aid interpretation of images obtained with any imaging modality.

Introduction

Diagnostic approaches in exotic pet medicine have evolved over the past 2 decades[1]; however, diagnosis of disease in pet birds remains difficult because captive birds usually maintain some inherited protective instincts, such as hiding signs of illness. In such a scenario, diagnostic testing is an important component of the clinical investigation. Diagnostic imaging in particular plays a fundamental role in avian medicine, and radiographic evaluation is often the first step in the diagnosis of lesions of the head of birds. Nevertheless, the small dimensions of the head in most avian species, along with the limited spatial resolution and the superimposition of several structures, often makes interpretation of plain radiographs challenging. By comparison, a 3-D imaging technique such as CT enables a higher spatial resolution and is particularly valuable in the evaluation of complex structures, such as the bones of the head[1]. Furthermore, IV administration of contrast medium prior to CT image acquisition allows thorough evaluation of healthy and diseased soft tissues.

Computed tomography is now routinely performed in dogs and cats, and a large amount of reference material is available on this subject[2]. The lack of available references regarding normal and pathological CT features of exotic animals may deter some clinicians from using CT when attempting to diagnose disease in these patients. To partially overcome this limitation, the normal CT anatomy of several exotic species has been published in the last decade[3–14]. The normal CT features of eyes[15,16] and paranasal sinuses[17] in some parrot species have already been published. However, to the best of the authors' knowledge, a comprehensive description of the normal CT anatomy of structures of the head is unavailable for parrot species.

The purpose of the study reported here was to develop a series of images of the normal cross-sectional anatomy (evaluated through different dissection planes) and corresponding contrast-enhanced CT features of the head in 3 common pet parrot species: blue-and-gold macaw (Ara ararauna), African grey parrot (Psittacus erithacus), and monk parakeet (Myiopsitta monachus). A secondary aim was to summarize the most appropriate window width and window level (window) values as well as the CT reconstruction kernels (filter) with which to evaluate various structures or organs of the head.

Material and Methods

Animals

For the CT portion of the study, 3 live blue-and-gold macaws (2 males and 1 female; mean ± SE body weight, 1,002 ± 16 g; mean body length, 85 ± 3 cm), 5 African grey parrots (3 males and 2 females; mean body weight, 369 ± 7 g; mean body length, 34.5 ± 2 cm), and 6 monk parakeets (3 males and 3 females; mean body weight, 129 ± 3 g; mean body length, 29 ± 1 cm) that were brought to the Veterinary Teaching Hospital of the University of Padova

in Padua, Italy from May 2015 through August 2015 were enrolled. The birds had been part of a study of the prevalence of subclinical airway infections in captivity-kept parrots. All had undergone CT examination of their entire body as part of their diagnostic work-up, and no lesions of the head were identified. This study was carried out with the approval of the University of Padua Ethical Committee (OPBA): Protocol No. 116052; April 28, 2015. Written owner consent was obtained for each patient.

For the anatomic evaluation portion of the study, the cadavers of 4 adult blue-and-gold macaws (1 male and 3 female; mean ¬± SE body weight, 1,000 ± 15 g; mean body length, 84 ± 2 cm), 4 adult African grey parrots (2 male and 2 female; mean body weight, 346 ± 4 g; mean body length, 33 ±1.5 cm), and 7 monk parakeets (3 male and 4 female; mean weight, 128 ± 2 g; mean body length, 28.5 ± 0.5 cm) were used. All cadavers had been donated by owners to the Veterinary Teaching Hospital of the University of Padova or to the Clinic for Exotic Animals in Rome, Italy. The birds had been referred to these institutions from September 2014 through August 2015 for specialty examination and died soon after hospitalization or were euthanized because of advanced medical conditions. Eight birds had had hepatic insufficiency, 4 had had egg retention, and 3 had had renal failure; none of these diseases directly involved the head. Cadavers were stored immediately after death at –20°C, in the same position as the live birds were positioned in during CT examination until completely frozen (48 to 72 hours, depending on size).

CT imaging

Each bird was anesthetized for CT examination with sevofluranea and oxygen delivered via a face mask. The trachea was then intubated with an appropriate endotracheal tube, and anesthesia was maintained with sevoflurane carried by a mixture of air and oxygen.

Birds were positioned in a prone position and kept still by means of a foam cradle. Imaging was performed in a craniocaudal direction by use of a 4-multidetector-row CT scannerb in helical acquisition mode, with an exposure time of 0.725 seconds, voltage of 120 kV, amperage of 150 mA, and slice thickness of 1 mm (reconstruction interval, 0.8 mm). After precontrast images were acquired, contrast mediumc (660 mg/kg) was injected in the right jugular vein with a 28-gauge needle, and imaging was repeated as fast as possible. Standard and contrast-enhanced CT images were reconstructed with a standard soft tissue filter with beam-hardening correction processing (setting Fc10) and a high-resolution filter for the inner ear and bones (setting Fc81), and displayed in a bone window (window length, 1,000 HU; window width, 4,000 HU), pulmonary window (window length, –500 HU; window width, 1,400 HU), and soft tissue window (window length, 40 HU; window width, 350 HU).

Anatomical procedures

Freshly frozen cadavers were sectioned into 5-mm consecutive slices with an electric band saw, from the cranial portion of the rhamphotheca to the caudal aspect of the neck. The slices were then numbered, cleaned with water, and photographed on both sides. A general inspection of the slices was performed to rule out any apparent pathological abnormality.

Labeling of CT and photographic images

Existing anatomic references18–21 were used to identify and label anatomic structures in photographs of cadaveric cross-sections. Photographs of cross-sections were then matched with the corresponding CT images, and CT images were labeled on the basis of the information provided in the corresponding photographs.

Results

Postcontrast CT images obtained from live parrot species and photographs of anatomic cross-sections obtained from cadaveric parrot species were reviewed, and representative images with the best diagnostic quality were selected (Figures 1–8). Most of the clinically relevant structures of the head were visible in both the cross-sections and corresponding CT images. Generally, a high degree of correspondence between anatomic structures visible in the 2 sets of images was observed. The most useful filters and windows with which optimal visibility of the various head structures was achieved via CT were summarized (Table 1).

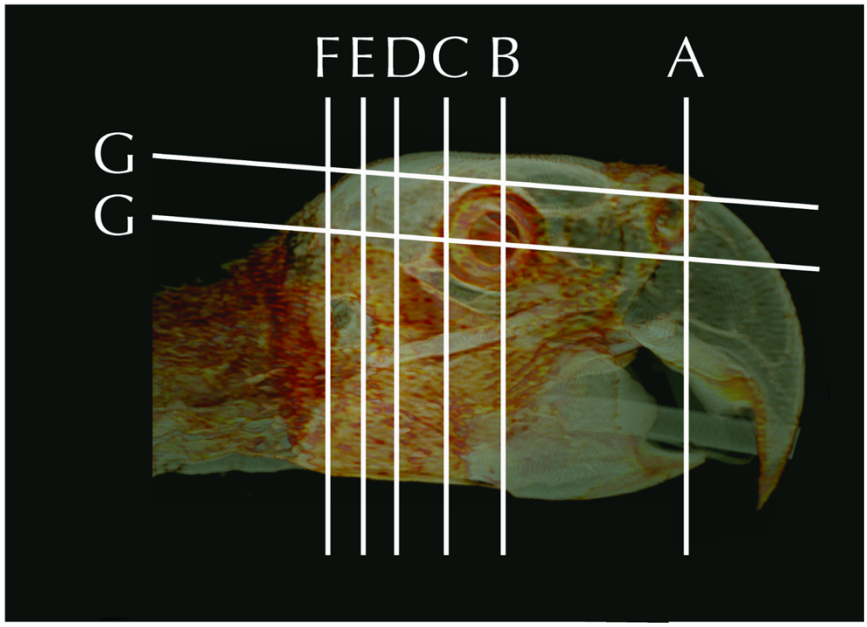

Figure 1 - Three-dimensional CT reconstruction image of the head of a blue-and-gold macaw (Ara ararauna), with labeled lines indicating the level

The thin trabeculae characterizing the avian skull were optimally visible on CT images when a standard soft tissue filter and pulmonary window was used (Figure 2). The same CT settings allowed clear visualization of the nostrils, operculum, infraorbital sinus, and cervicocephalic air sacs. The sinus and the air sacs were visible as air-filled spaces bordered by the adjacent structures[22–24] (Figures 2–8).

A standard soft tissue filter with a soft tissue window allowed a good visibility of the eyes

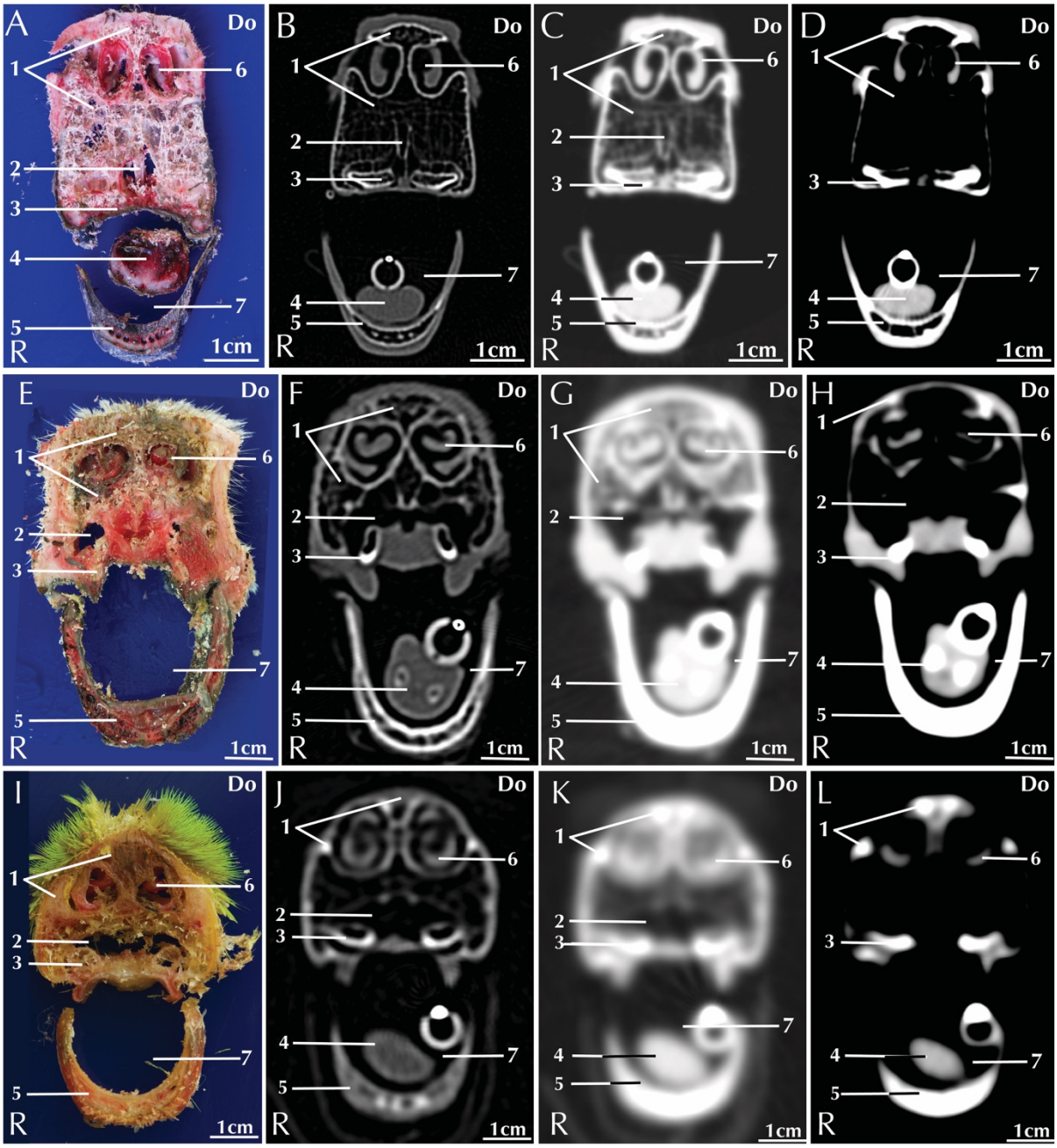

and related structures in all examined parrot species (Figures 3 and 4).

Figure 2 - Representative photographs of anatomic cross sections (A, E, and I) and matched CT images at the level of the nostrils (corresponding to line A in Figure 1) of the head of a blue-and-gold macaw (A–D), African grey parrot (*E*–H), and monk parakeet (*I*–L). The CT images were reconstructed with a high-resolution filter and displayed in a bone window (window length, 1,000 HU; window width, 4,000 HU; B, F, and J) or with a standard soft tissue filter and displayed in a pulmonary window (window length, –500 HU; window width, 1,400 HU; C, G, and K) or soft tissue window (window length, 40 HU; window width, 350 HU; D, H, and L). 1 = Premaxillary bone. 2 = Preorbital diverticulum of the infraorbital sinus. 3 = Palatine bone. 4 = Tongue. 5 = Mandible. 6 = Medial nasal concha. 7 = Oral cavity. Do = Dorsal. R = Right.

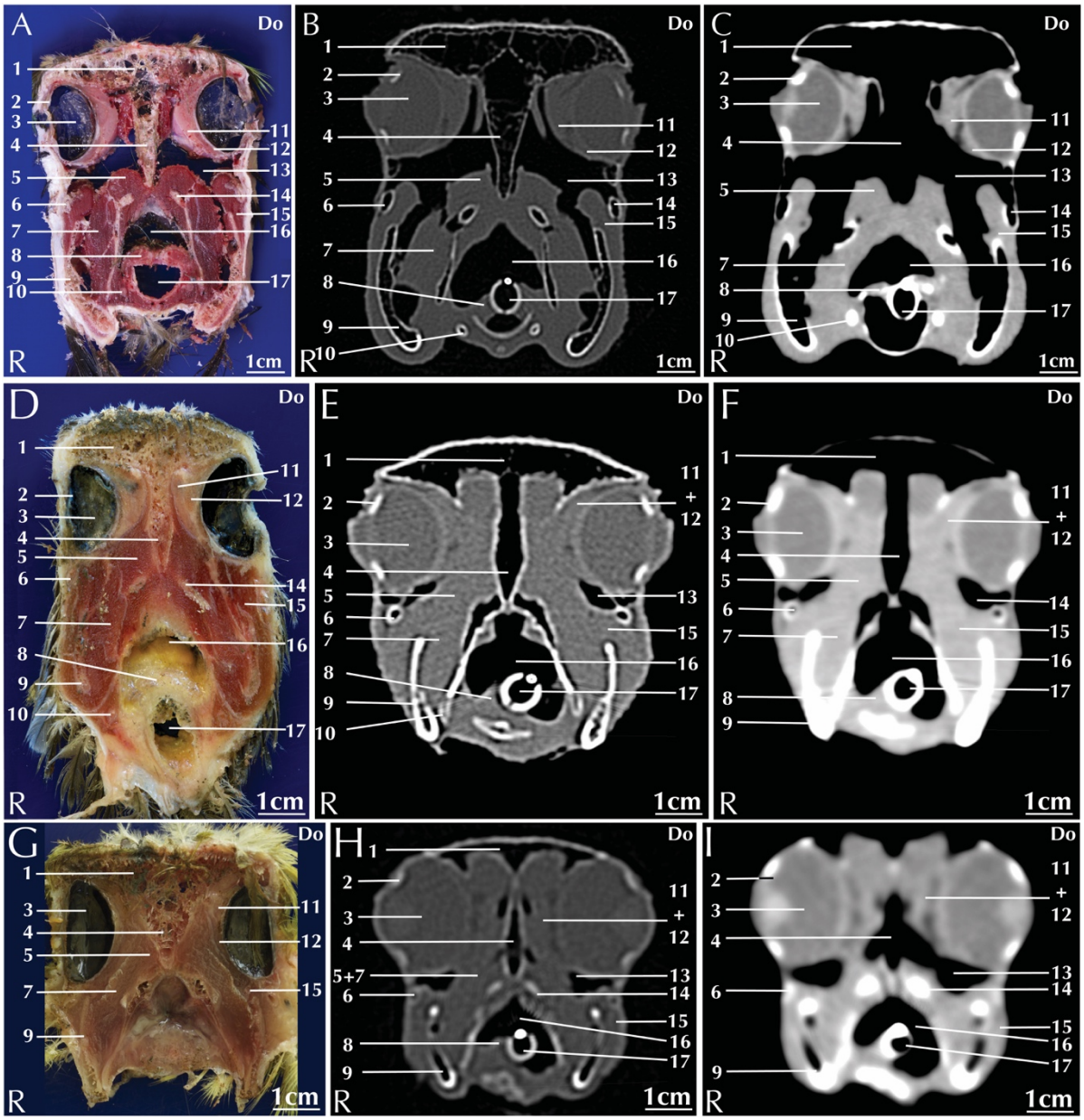

Figure 3—Representative photographs of anatomic cross sections (A, D, and G) and matched CT images at the level of the nostrils (corresponding to line B in Figure 1) of the head of a blue-and-gold macaw (A–C), African grey parrot (D–F), and monk parakeet (G–I). The CT images were reconstructed with a high-resolution filter and displayed in a bone window (window length, 1,000 HU; window width, 4,000 HU; B, E, and H) or with a standard soft tissue filter and displayed in a soft tissue window (window length, 40 HU; window width, 350 HU; C, F, and I). 1 = Frontoparietal bone. 2 = Scleral ossicle. 3 = Vitreous chamber of the eye. 4 = Septum interorbitale. 5 = Musculus ethmomandibularis. 6 = Suborbital arch. 7 = Musculus adductor mandibulae externus ventralis. 8 = Glottis. 9 = Mandible. 10 = Ceratobranchiale. 11 = Gland of nictitating membrane. 12 = Musculus medial rectus. 13 = Infraorbital diverticulum of the infraorbital sinus. 14 = Pterygoid bone. 15 = Venter externus of musculus pterygoideus ventralis lateralis. 16 = Oral cavity. 17 = Trachea (endotracheal tube is visible). 18 = Mandible. Do = Dorsal. R = Right.

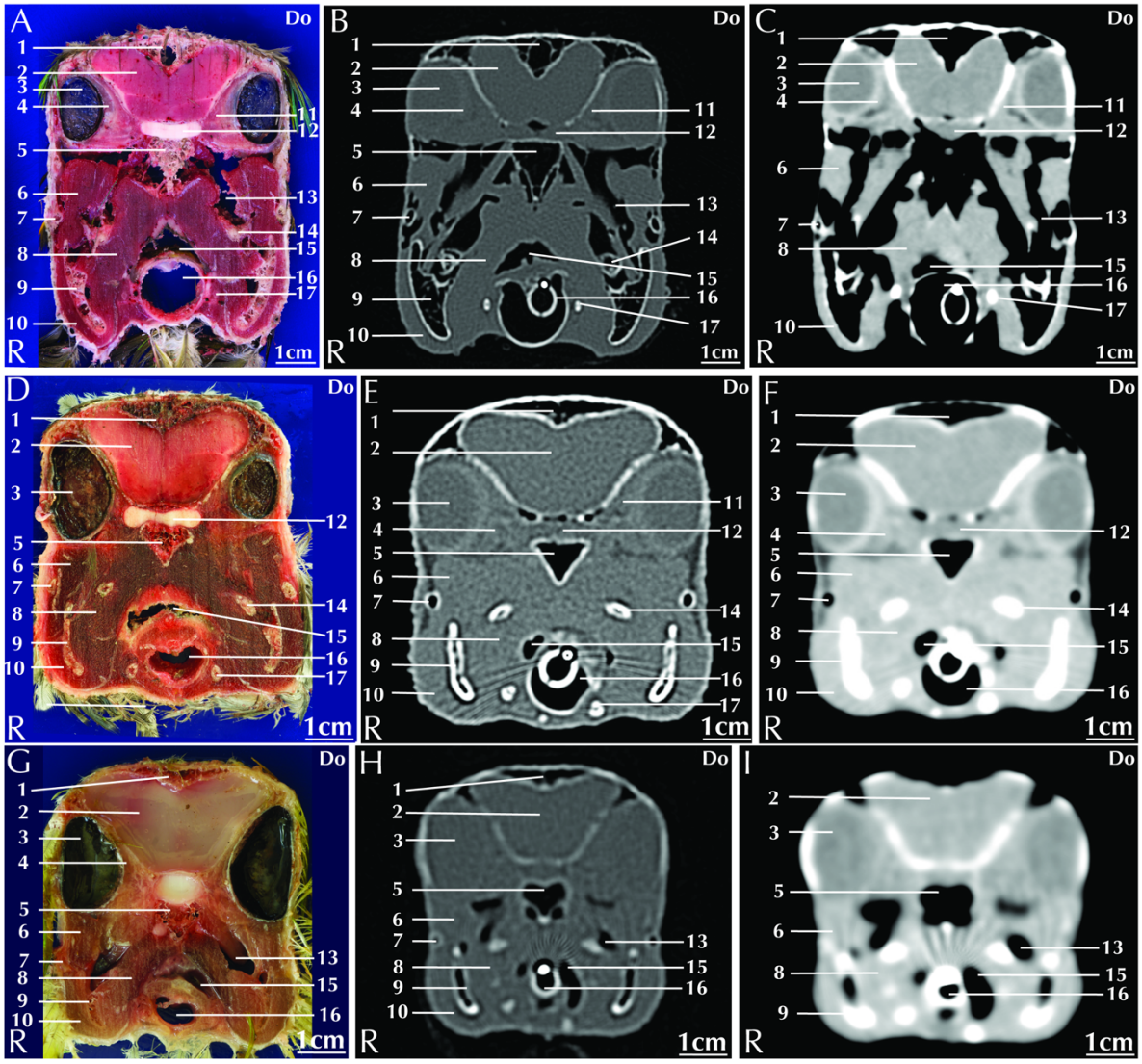

Figure 4—Representative photographs of anatomic cross sections (A, D, and G) and matched CT images at the level of the nostrils (corresponding to line C in Figure 1) of the head of a blue-and-gold macaw (A–C), African grey parrot (D–F), and monk parakeet (G–I). 1 = Frontoparietal bone. 2 = Brain, frontal portion of the telencephalon. 3 = Vitreous chamber of the eye. 4 = Gland of nictitating membrane. 5 = Septum interorbitale. 6 = Venter externus of musculus pterygoideus ventralis lateralis. 7 = Jugal bone. 8 = Musculus adductor mandibulae externus ventralis. 9 = Mandible. 10 = Musculus pterygoideus ventralis lateralis. 11 = Musculus dorsal oblique. 12 = Optic nerve. 13 = Infraorbital diverticulum of the infraorbital sinus. 14 = Pterygoid bone. 15 = Oral cavity. 16 = Trachea. 17 = Ceratobranchiale. See Figure 3 for remainder of key.

The anterior chamber was clearly distinguishable from the hyperattenuating lens in the lateralmost portion of the eye.The scleral ossicles were visible as mineral-attenuating structures in the intermediate segment. The vitreous chamber could be perceived as a semispherical structure filling most of the orbit. The retina and chorioid were distinguishable

as a single contrast enhancing line. The gland of the nictitating membrane was visible in both the CT images and the anatomic cross-sections, whereas the lacrimal glands could not be identified. The ocular muscles were discernible in both the CT images and the anatomic cross-sections.

The optic nerves were clearly visible as elongated structures running from the caudal portion of the eye to the midline of the head, where they connected to form the optic chiasm[15,16,22–26] (Figure 5).

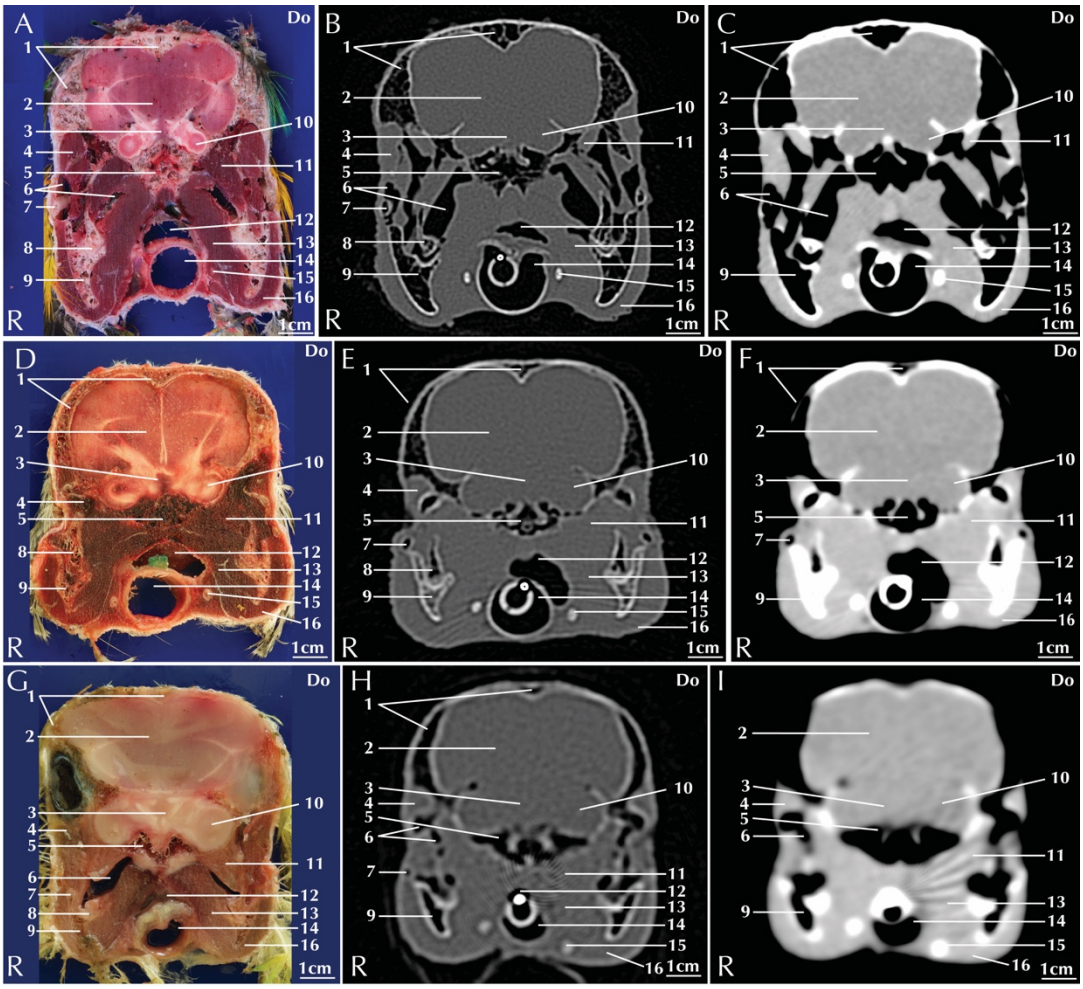

Figure 5 - Representative photographs of anatomic cross sections (A, D, and G) and matched CT images at the level of the nostrils (corresponding to line D in Figure 1) of the head of a blue-and-gold macaw (A–C), African grey parrot (D–F), and monk parakeet (G–I). 1 = Frontoparietal bone. 2 = Brain, parietal part. 3 = Optic chiasm. 4 = Venter externus of Musculus pterygoideus ventralis lateralis. 5 = Basisphenoid bone. 6 = Postorbital diverticula of the infraorbital sinus. 7 = Jugal bone. 8 = Quadrate bone. 9= Mandible. 10 = Midbrain. 11 = Musculus adductor mandibulae externus rostralis temporalis. 12 = Oral cavity. 13 = Musculus pterygoideus ventralis medialis. 14 = Trachea. 15 = Ceratobranchiale. 16 = Musculus adductor mandibulae externus ventralis. See Figure 3 for remainder of key.

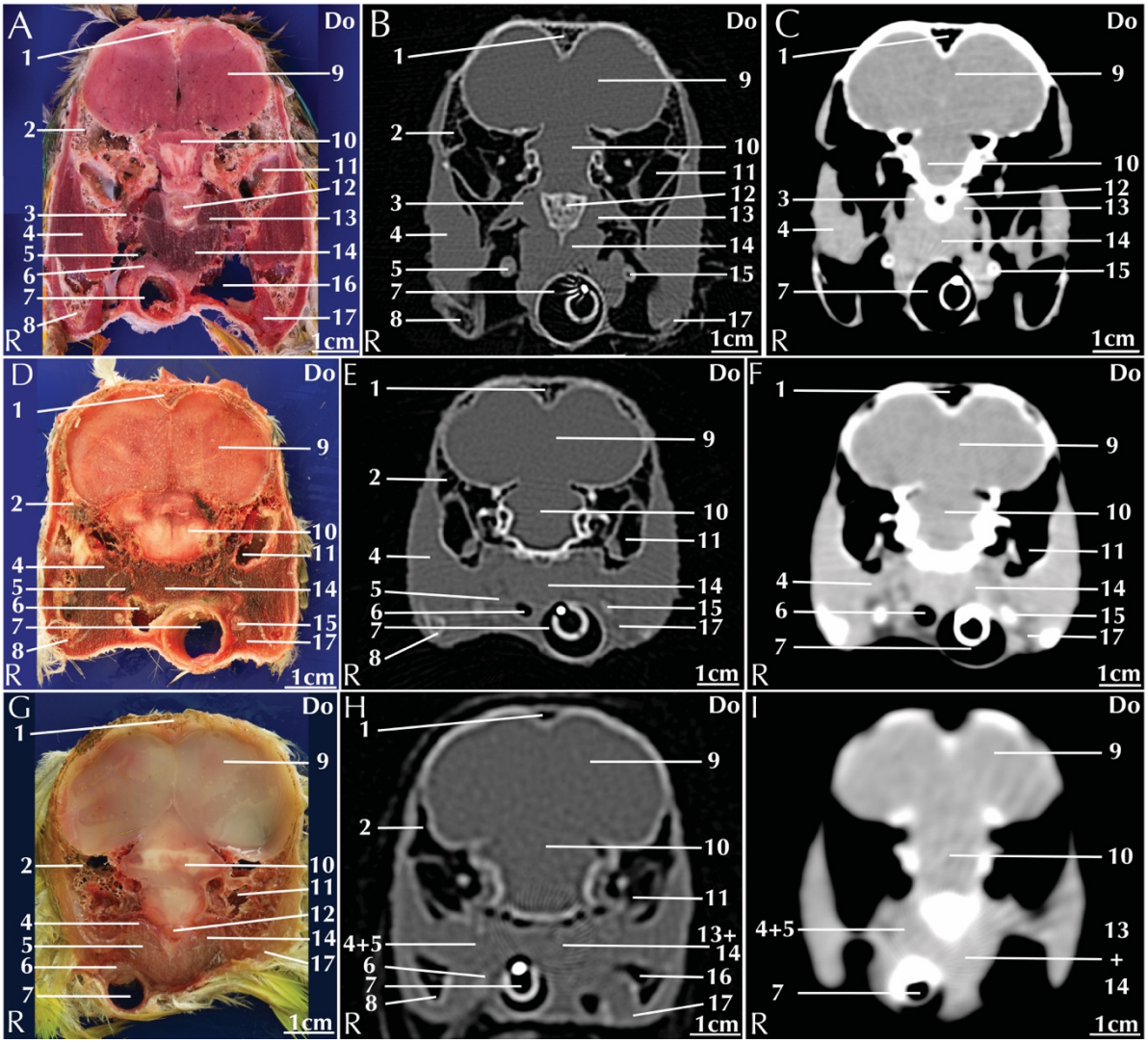

Figure 6 - Representative photographs of anatomic cross sections (A, D, and G) and matched CT images at the level of the nostrils (corresponding to line E in Figure 1) of the head of a blue-and-gold macaw (A–C), African grey parrot (D–F), and monk parakeet (G–I). 1 = Frontoparietal bone. 2 = Postorbital process. 3 = Musculus adductor mandibulae externus rostralis temporalis. 4 = Venter externus of musculus pterygoideus ventralis lateralis. 5 = Jugular vein. 6 = Esophagus. 7 = Trachea. 8 = Mandible. 9 = Brain, parietal portion. 10 = Cerebellum. 11 = Ear canal. 12 = Vertebra. 13 = Musculus intertransversarii. 14 = Musculus flexor colli medialis. 15 = Ceratobranchiale. 16 = Mandibular diverticulum of the infraorbital sinus. 17 = Musculus adductor mandibulae externus ventralis. See Figure 3 for remainder of key.

Optic nerves in birds are relatively large structures, and in some species, they can measure as large as half the diameter of the spinal cord. The cerebral hemispheres, cerebellum, and medulla oblongata were distinguishable only on anatomic cross-sections, and all had the same soft tissue attenuation (Figures 5–7).

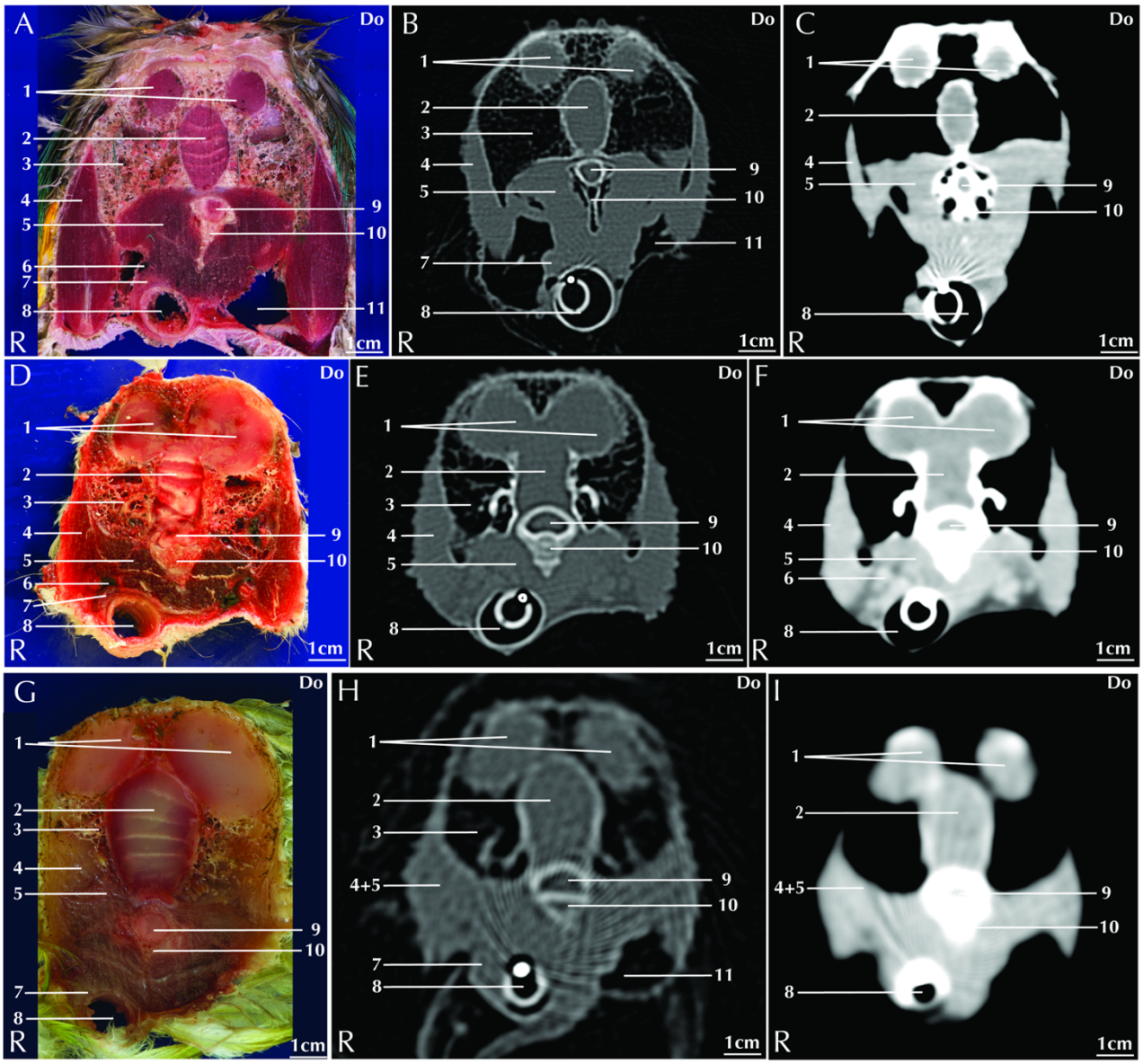

Figure 7 - Representative photographs of anatomic cross sections (A, D, and G) and matched CT images at the level of the nostrils (corresponding to line F in Figure 1) of the head of a blue-and-gold macaw (A–C), African grey parrot (D–F), and monk parakeet (G–I). 1 = Brain, occipital part. 2 = Cerebellum. 3 = Occipital bone. 4 = Venter externus of musculus pterygoideus ventralis lateralis. 5 = Musculus flexor colli medialis. 6 = Jugular vein. 7 = Esophagus. 8 = Trachea. 9 = Spinal cord. 10 = Vertebra. 11 = Mandibular diverticulum of the infraorbital sinus. See Figure 3 for remainder of key.

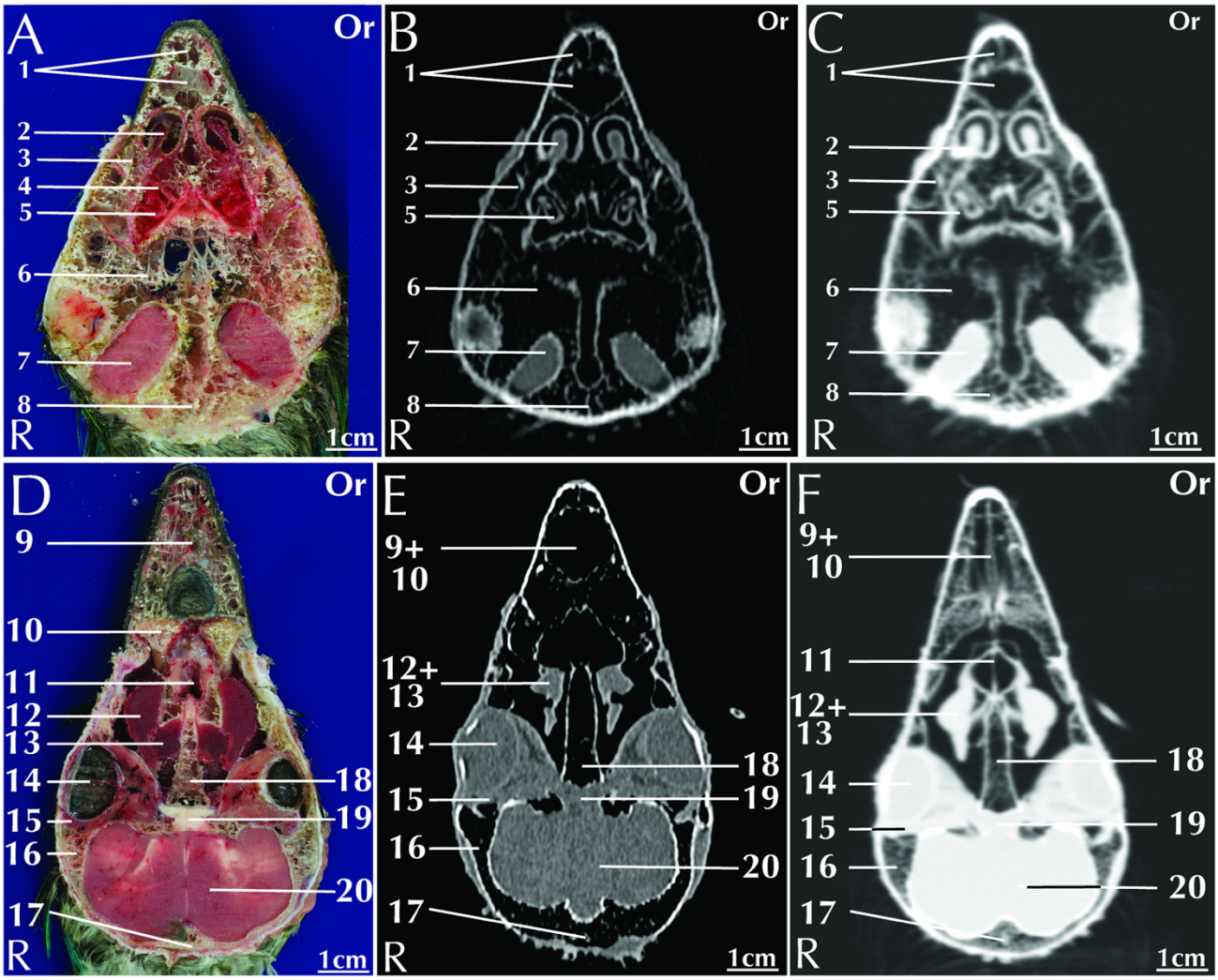

Figure 8 - Representative photographs of anatomic cross sections (A and D) and matched CT images at the level of the nostrils (corresponding to lines G and H in Figure 1) of the head of a blue-and-gold macaw (body weight, 1,010 g; body length, 86 cm) in the dorsal plane. The CT images were reconstructed with a high-resolution filter and displayed in a bone window (window length, 1,000 HU; window width, 4,000 HU; B and E) or with a standard soft tissue filter and displayed in a soft tissue window (window length, 40 HU; window width, 350 HU; C and F). 1 = Rostral diverticulum of the infraorbital sinus. 2 = Cranial nasal concha. 3 = Nasal bone. 4 = Medium nasal concha. 5 = Caudal nasal concha. 6 = Parietal bone. 7 = Brain, occipital part. 8 = Supraoccipital bone. 9 = Premaxilla. 10 = Maxilla. 11 = Choana. 12 = Musculus pterygoideus. 13 = Musculus ethmomandibularis. 14 = Eye. 15 = Gland of the nictitating membrane. 16 = Temporal bone. 17 = Occipital bone. 18 = Interorbital septum. 19 = Optic nerve. 20 = Brain. Or = Orad. R = Right.

Discussion

In avian species, the head is characterized by the presence of pneumatized bones that are in direct connection with the paranasal sinus and the cervicocephalic air sacs[22]. We believe that the best CT imaging results regarding these structures were achieved by means of a pulmonary window in the present study because of the hypoattenuating nature of the trabeculae to bone when the bone window was used. Furthermore, reconstruction of CT images in a dorsal plane enabled a more comprehensive visual examination of some complex head structures, such as the diverticula of the infraorbital sinus and the periorbital muscles and glands (Figure 8).

A parrots' head can be affected by several pathological processes. Trauma caused by fights, household accidents, or other causes1 are common complaints of parrot owners. Severe mycotic or bacterial infections, involving several structures of the head of pet parrots, have been reported[27,28]. Neoplastic disease such as lymphosarcoma, mast cell tumor, fibroma, papilloma, hemangiosarcoma, and osteosarcoma originating from head structures of avian species have been reported[22–29,30], as have congenital disorders, such as hydrocephalus or beak deformities[22,31,32].

An important aspect of the anatomy of the heads of birds is the proximity of the paranasal sinus to the orbit. Sinusitis with subsequent enlargement of the paranasal sinus can cause a compression of the orbit, periocular swelling, conjunctivitis, and sometimes intraocular disease[22]. Ultrasonographic examination is the most commonly used imaging technique to evaluate birds' intraocular structures[15,16]. Nevertheless, ultrasonographic examination is limited to the ocular globe and optic nerve, and the scleral ossicles are better examined by means of CT. The combination of the 2 imaging techniques might be recommended as the most suitable option for a complete evaluation of the eye and related structures[16].

The matched anatomic cross-sections and CT images created in the present study may serve as a useful reference for interpretation of diagnostic images of the head of the 3 parrot species evaluated. The CT procedure used was fast and safe, and most of the clinically relevant structures could be thoroughly evaluated. Moreover, the use of a contrast medium allowed optimal visibility of the soft tissues. Findings suggested that given complex nature of the avian head, combined with its small dimensions, CT would be the imaging technique of choice in the evaluation of lesions of the heads of birds. Findings regarding the optimal settings for CT examination of particular head structures (Table 1) also served as a reminder that assessment of anatomy and pathological characteristics via CT is dependent on optimizing acquisition algorithms, filters, and viewing parameters.

Table 1- List of the most useful CT reconstruction kernels (filter) and window widths and levels (window) with which diagnostic images of various anatomic structures in the heads of parrot species were obtained.

Head structure	Filter	Window
Basisphenoid and parsphenoid bone	High resolution	Bone
Brain	Soft tissue	Soft tissue
Ceratobranchiale	High resolution	Bone
Cerebellum	Soft tissue	Soft tissue
Ear canal	High resolution	Bone
Frontoparietal bone	High resolution	Bone
Gland of the nictitating membrane	Soft tissue	Soft tissue
Glottis	Soft tissue	Soft tissue
Hyoid skeleton	High resolution	Bone
Infraorbital sinus	Soft tissue	Pulmonary
Jugal bone	High resolution	Bone
Jugular vein	Soft tissue	Soft tissue
Lens of the eye	Soft tissue	Soft tissue
Muscles	Soft tissue	Soft tissue
Mandible	High resolution	Bone
Maxilla	High resolution	Bone
Medial nasal concha	Soft tissue	Pulmonary
Occipital bone	High resolution	Bone
Esophagus	Soft tissue	Soft tissue
Optic chiasm	Soft tissue	Soft tissue
Optic nerve	Soft tissue	Soft tissue
Oral cavity	Soft tissue	Soft tissue
Palatine bone	High resolution	Bone
Premaxillary bone	High resolution	Bone
Pterygoid bone	High resolution	Bone
Scleral ossicles	High resolution	Bone
Septum interorbitale	High resolution	Bone
Spinal cord	Soft tissue	Soft tissue
Suborbital arch	High resolution	Bone
Tongue	Soft tissue	Soft tissue
Trachea	Soft tissue	Soft tissue
Vertebra	High resolution	Bone
Vitreous chamber of the eye	Soft tissue	Soft tissue

Footnotes

a. SevoFlo, Abbott Laboratories Ltd, Maidenhead, United Kingdom.

b. Toshiba Asteion S4, Toshiba Medical System Europe, Zoetermeer, The Netherlands.

c. Optiray (350 mg/mL), Covidien Spa, Segrate, Italy.

References

1. Krautwald-Junghanns ME. Birds. In: Krautwald-Junghanns ME, Pees M, Reese S, Tully T, editors. Diagnostic imaging of exotic pets: Birds, small mammals, reptiles. Hannover, Germany: Schlutersche Verlagsgesellschaft mbH & Co, 2010. p.1–141.

2. d'Anjou MA. Principles of computed tomography and magnetic resonance imaging. In: Thrall DE, editor. Textbook of veterinary diagnostic radiology. St. Louis: Elsevier Saunders, 2013;50–73.

3. Alonso-Farré JM, Gonzalo-Orden M, Barreiro-Vázquez JD, Ajenjo J M., Barreiro-Lois A.,

Llarena-Reino M, et al. Cross-sectional anatomy, computed tomography and magnetic resonance imaging of the thoracic region of common dolphin (*Delphinus delphis*) and striped dolphin (*Stenella coeruleoalba*). Anat Histol Embryol 2014; 43:221–229.

4. Banzato T, Selleri P, Veladiano IA, Zotti A. Comparative evaluation of the cadaveric and computed tomographic features of the coelomic cavity in the green iguana (*Iguana iguana*), black and white tegu (*Tupinambis merianae*) and bearded dragon (*Pogona vitticeps*). Anat Histol Embryol 2013;42:453–460.

5. Banzato T, Russo, E, Toma A, Palmisano G., Zotti A. Evaluation of radiographic, computed tomographic, and cadaveric anatomy of the head of boa constrictors. Am J Vet Res 2011;72:1592–1599.

6. Banzato T, Selleri P, Veladiano I, Martin A, Zanetti E, Zotti A. Comparative evaluation of the cadaveric, radiographic and computed tomographic anatomy of the heads of green iguana (*Iguana iguana*), common tegu (*Tupinambis merianae*) and bearded dragon (*Pogona vitticeps*). BMC Vet Res 2012;8:53.

7. de Rycke LM, Boone MN, van Caelenberg AI, Dierick M, Van Hoorebeke L, van Bree H, et al. Micro–computed tomography of the head and dentition in cadavers of clinically normal rabbits. Am J Vet Res 2012;73:227–232.

8. Endo H, Sasaki H, Hayashi Y, Petrov EA, Amano M, Suzuki N et al. CT examination of the head of the baikal seal (*Phoca sibirica*). J Anat 1999;194:119–126.

9. Gumpenberger M, Henninger W. The use of computed tomography in avian and reptile medicine. Semin Avian and Exot Pet Med 2001;10:174–180.

10. Krautwald-Junghanns ME, Kostka V, Dorsch B. Comparative studies on the diagnostic value of conventional radiography and computed tomography in evaluating the heads of psittacine and raptorial birds. J Avian Med Surg 1998;12:149–157.

11. Krautwald-Junghanns ME, Valerius K, Duncker H, Sohn HG. CT-assisted versus silicone rubber cast morphometry of the lower respiratory tract in healthy amazons (Genus amazona) and grey parrots (Genus psittacus). Res Vet Sci 1998;65:17–22.

12. Orsoz S, Toal R. Tomographyc anatomy of the golden eagle (*Aquila chrysaetos*). J Zoo Wildl Med 1992;23:39–46.

13. Pepperberg IM, Howell KS, Banta PA, Patterson DK, Meister M. Measurement of grey parrot (*Psittacus erithacus*) trachea via magnetic resonance imaging, dissection, and electron beam computed tomography. J Morphol 1998;238:81–91.

14. Zotti A, Banzato T, Cozzi B. Cross-sectional anatomy of the rabbit neck and trunk: Comparison of computed tomography and cadaver anatomy. Res Vet Sci 2009;87:171–176.

15. Bayòn A, Almela RM, Talavera J. Avian ophthalmology. Eur J Compan Anim Pract 2007;17:1–13.

16. Gumpenberger M, Kolm G. Ultrasonographic and computed tomographic examinations of the avian eye: physiologic appearance, pathologicalfindings, and comparative biometric measurement. Vet Radiol Ultrasound 2006;47:492–502.

17. Artmann A, Henninger W. Psittacine paranasal sinus a new definition of compartments. J Zoo Wildl Med 2001;32:447–458.

18. Burton PJK. Jaw and tongue features in psittaciformes and other orders with special reference to the anatomy of the tooth-billed pigeon (*Didunculus strigirostris*). J Zool 1974;174:255–276.

19. Carril J, Tambussi CP, Degrange F, Benitez Saldivar MJ, Picasso MBJ. Comparative brain morphology of neotropical parrots (Aves, psittaciformes) inferred from virtual 3D endocasts. J Anat 2015 [Epub ahead of print].

20. Dumont ER. Bone density and the lightweight skeletons of birds. Proc Royal Soc Lond B Bio 2010; 277:2193–2198.

21. Huang R, Zhi Q, Izpisua-Belmonte J, Christ B, Patel K. Origin and development of the avian tongue muscles. Anat Embryol 1999;200:137–152.

22. Harrison GJ, Harrison LR. Clinical avian medicine and surgery, including aviculture. Philadelphia: WB Saunders Co, 1986:1-717.

23. Williams D. Ophtalmology. In: Ritchie BW, Harrison GJ, Harrison LR, editors. Avian medicine, principle and applications. Lake Worth, FL: Wingers Publishing Inc, 1994;673-677.

24. Cole BH. Avian medicine and surgery. Oxford: Blackwell Science;1997; 1-408.

25. Heard DJ. Avian respiratory anatomy and physiology. Semin Avian Exot Pet 1997;10:172–179.

26. Bellairs A. The early development of the interorbital septum and the fate of the anterior orbital cartilages in birds. J Embryol Exp Morphol 1958;6:68–85.

27. Diaz-Figueroa O, Tully Jr. TN, Williams J, Evans D. Squamous cell carcinoma of the infraorbital sinus with fungal tracheitis and ingluvitis in an adult Solomon eclectus parrot (*Eclectus roratus solomonensis*). J Avian Med Surg 2006;20:113–119.

28. Raidal S, Butler R. Chronic rhinosinusitis and rhamphothecal destruction in a Major Mitchell's cockatoo (*Cacatua leadbeateri*) due to cryptococcus neoformans var gattii. J Avian Med Surg 2001;15:121–125.

29. Baine K, Nobrega-Lee M, Jones MP, Steeil J, McCleery B, Ramsay E, et al. Branchial cyst with carcinoma in an umbrella cockatoo (*Cacatua alba*). J Avian Med Surg 2014 Sep;28:232–239.

30. Riddell C, Cribb PH. Fibrosarcoma in an African grey parrot (*Psittacus erithacus*). Avian Dis 1983;27:549.

31. Johnston HA, Lindstrom JG, Oglesbee M. Communicating hydrocephalus in a mature Goffin's cockatoo (*Cacatua goffini*). J Avian Med Surg 2006;20:180–184.

32. Keller KA, Guzman DS, Muthuswamy A, Forrest LJ, Steinberg H, Sladky K, et al. Hydrocephalus in a yellow-headed Amazon parrot (*Amazona ochrocephala oratrix*). J Avian Med Surg 2011;25:216–224.

Chapter V: Normal computed tomographic features and reference values for the coelomic cavity in pet parrots

This chapter is adapted from: Veladiano I.A., Banzato T., Bellini L., Montani A., Catania S., Zotti A. Normal computed tomographic features and reference values for the coelomic cavity in pet parrots. BMC Veterinary Research 2016 12:182

Abstract

The increasing popularity gained by pet birds over recent decades has highlighted the role of avian medicine and surgery in the global veterinary scenario; such a need for speciality avian medical practice reflects the rising expectation for high-standard diagnostic imaging procedures. The aim of this study is to provide an atlas of matched anatomical cross-sections and contrast-enhanced CT images of the coelomic cavity in three highly diffused psittacine species.

Contrast-enhanced computed tomographic studies of the coelomic cavity were performed in 5 blue-and-gold macaws, 4 African grey parrots and 6 monk parakeets by means of a 4-multidetector-row CT scanner. Both pre- and post-contrast scans were acquired. Anatomical reference cross-sections were obtained from 5 blue-and-gold macaw, 7 African grey parrot, and 9 monk parakeet cadavers. The specimens were stored in a -20°C freezer until completely frozen and then sliced at 5-mm intervals by means of a band saw. All the slices were photographed on both sides. Individual anatomical structures were identified by means

of the available literature. Pre- and post-contrast attenuation reference values for the main coelomic organs are reported in Hounsfield units (HU).

The results provide an atlas of matched anatomical cross-sections and contrast-enhanced CT images of the coelomic cavity in three highly diffused psittacine species.

Introduction

The increasing popularity gained by pet birds over recent decades has highlighted the role of avian medicine and surgery in the global veterinary scenario. The success of birds as pets is likely due both to the strong emotional connection linking such animals to their owners and to the high economical value of some species[1]. Among birds, psittacines have become one of the most diffused avian pet species; their appealing appearance, their deep interaction with the owner and the long lifespan expectation typical of some species represent the main reasons for their spread.

The increasing need for speciality avian medical procedures during recent decade reflects the rising expectation among owners for high-standard medical treatment for their pets.

Most parrots are so-called “stoic” animals; to avoid predation these animals evolved to mask signs of illness[2]. Accordingly, clinical signs are difficult to notice during routine examination, the role of ancillary diagnostic techniques becomes vital in the diagnosis of several different diseases.

Diagnostic imaging plays a key role in exotic pet medicine and several references aimed at standardizing normal features through different imaging techniques in exotic and wild mammals[3-8], reptiles[9-15], and birds[16-21] are currently available.

Some references describing the CT (computed tomographic) features of the coelomic cavity of avian species are currently available[16-21]. However, to the best of the authors’ knowledge,

no specific references regarding the coelomic cavity in psittacines have yet been published. Moreover, little information is available regarding the use of contrast medium to enhance the visibility of individual coelomic organs in avian patients [22].

The aim of this study is to provide an atlas of matched anatomical cross-sections and contrast-enhanced CT images of the coelomic cavity in three highly diffused psittacine species (monk parakeet, African grey parrot, and blue-and-gold macaw). In addition, pre- and post-contrast attenuation reference values for the main coelomic organs are reported in Hounsfield units (HU).

Material and Methods

Animals

Three different species of parrots were selected for the present study: blue-and-gold macaw (Ara ararauna), African grey parrot (Pittacus erithacus) and monk parakeet (Myiopsitta monachus). 5 blue-and-gold macaws (2 males and 3 females, mean weight 1000gr ± 14gr, mean length 86cm ± 3.5cm), 4 African grey parrots (3 males and 1 females, mean weight 371gr ± 5gr, mean length 35cm ± 1.5cm) and 6 monk parakeets (3 males and 3 females, mean weight 130gr ± 2.5gr, mean length 28.5cm ± 1cm) presented to the University Veterinary Teaching Hospital of the University of Padua (Padua, Italy) were included in the study*. All the animals enrolled for the study were affected by head or limb pathologies (7 head traumas and 8 leg fractures). Upon owner consent, whole body CT scans were performed.

Anatomical procedures

The cadavers of 5 adult-blue-and-gold macaws (3 males and 2 females, mean weight 1003gr ± 13.5gr, mean length 85cm ± 2cm), 7 adult African grey parrots (3 males and 4 females, mean weight 345gr ± 4.5, mean length 32 ± 2cm), and 9 monk parakeets (6 males and 3 females, mean weight 126gr ± 3gr, mean length 29 ± 0.5cm) were used in this study. Within 24-36 hours of death the cadavers were fixed in prone position on a plastic support and stored in a freezer (-20°C) for 48 hours. Consecutive 5-mm transverse slices were obtained by means of an electric band saw, from the inlet of the coelomic cavity to the cloaca. The slices were then numbered, cleaned with water and photographed on both sides. All the above animals died soon after hospitalization or were euthanized because of advanced medical conditions and their bodies were donated to the Veterinary Teaching Hospital of the University of Padua (Padua, Italy) or to the Clinic for Exotic Animals (Rome, Italy) by the owners.

Imaging procedures

Computed tomography examinations were performed by means of a 4-multidetector-row CT scanner (Asteion S4, Toshiba Medical System, Amsterdam, NL). All live animals were anaesthetized with sevoflurane and oxygen administered via a facial mask, then intubated with an appropriate endotracheal tube; anaesthesia was maintained with sevoflurane carried by a mixture of medical air and oxygen. Computed tomographic studies were performed following a cranio-caudal direction with the animal in a prone position. Pre- and post-contrast sequences were acquired. Contrast medium (Optiray® 350 mg/ml, Covidien Spa, Italy) was injected in the right jugular vein with a 28-gauge needle at a dose of 660 mg/kg. The CT parameters were: helical acquisition mode, exposure time of 0.725 seconds, voltage of 120 kV, amperage of 150 mA, slice thickness of 1 mm.

The images were reconstructed with a soft tissue kernel and displayed in bone (window length 1000, window width 4000), pulmonary (window length -500, window width 1400) and abdomen (window length 40, window width 350) windows.

Attenuation was measured in Hounsfield units (HU) in the lungs, air sacs, liver, spleen, ventriculus, intestine and kidney in pre- and post-contrast scans using a commercially available DICOM processing software (Osirix, pixmeo SARL, Switzerland). Measurements were repeated three times using a region of interest of the same dimensions both in the pre and post-contrast images, and then averaged.

Statistical analysis

Normality was graphically assessed by means of the Q-Q plot. Normally distributed data were reported as mean ± standard deviation whereas non-normally distributed variables were reported as median with the limits for the overall range. Differences among species were calculated through analysis of variance (ANOVA) in normally distributed data whereas differences were calculated utilizing the Kruskal-Wallis H Test in the non-normally distributed data.

Results

All the CT scans were performed on live animals and therefore a direct comparison with the anatomical images was not possible; nevertheless, visual inspections reveal a high correlation of both as shown in Figures 1 to 6.

Only post-contrast images are displayed. Individual anatomic structures were identified and labelled on the basis of the anatomical references[23-24-25], both in the anatomical cross-sections and in the corresponding CT images. All the main organs of the respiratory, digestive, urinary (including the ureters) and reproductive systems were visible both in the anatomical sections and in the corresponding CT images.

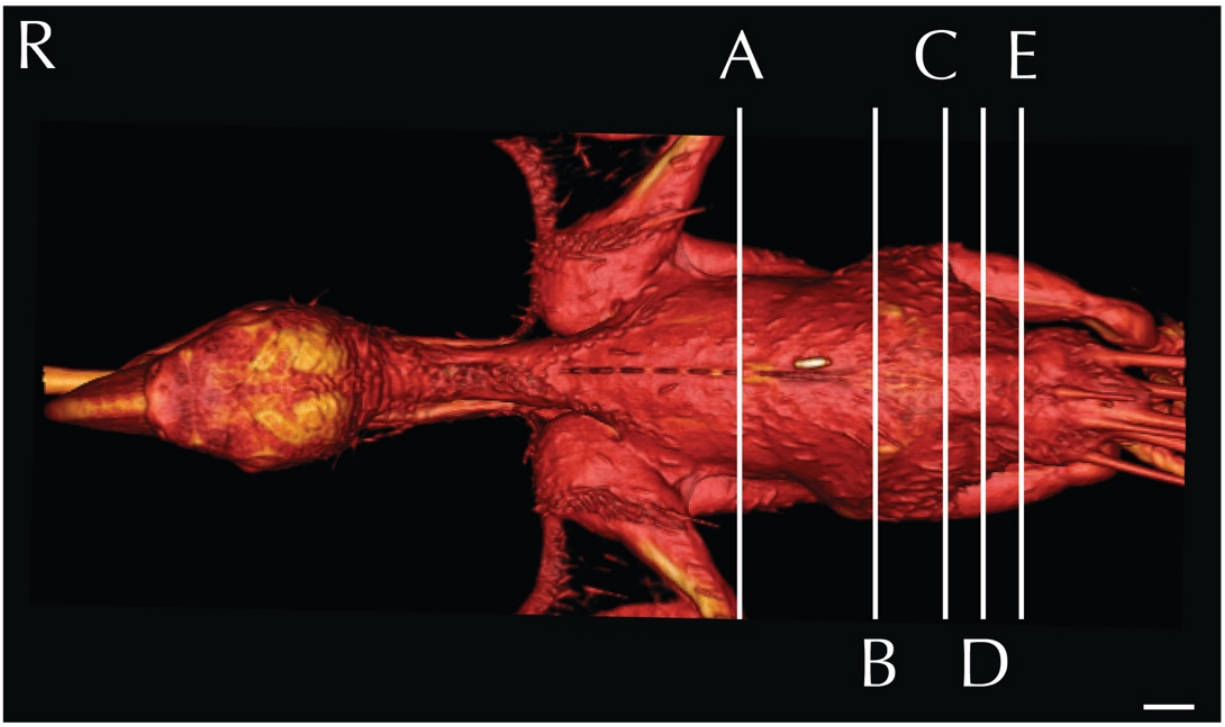

Fig. 1 - Three-dimensional reconstruction of the body of a blue-and-gold macaw. Lines A-E indicate the level of the matched cross-sections and CT images displayed in Figs. 2, 3, 4, 5, 6 and 7

The approximate level of the reported matching cross-sections and CT images are shown in Figure 1. The displayed matched cross-sectional images and CT scans shown in Figures 2-7 are approximately at the same level in all the considered species, and the same structures are present in almost all the corresponding slices of different species.

All the considered HU values were non-normally distributed; hence the differences among species were calculated by means of the Kruskal-Wallis H test. As no statistically significant differences among species were evident for any organ, only descriptive statistics of the pooled data have been reported. Medians with the limits for the overall range of HU values, for the selected coelomic organs are reported in Table 1.

Discussion

The coelomic cavity in the avian species is a single cavity with no further partitioning. Most of the coelomic cavity is filled by a very complex respiratory system that is composed of nine air sacs, six of which are in the coelomic cavity, plus two relatively small and non-expandable lungs.

The air sacs are air-filled structures covered by a thin pavimentous or cubical epithelium. This epithelium was clearly visible in CT scans of the blue-and-gold macaw and in the African grey parrot, but was not visible in monk parakeet (likely due to the small size of the animal) (Figs. 3B, 3E, 3H, 4B, 4E, 4H). The very limited vascularization of these structures brings differences that are undetectable between pre- and post-contrast scans[26].

The lungs are located cranio-dorsally in the coelomic cavity and are attached dorsally to vertebrae and ribs so that impressions of the ribs can be seen in isolated lung specimens[26]. These features were clearly visible in all the CT scans displayed in a pulmonary window (Figs. 2B, 2E, 2H). The trachea, the mainstem bronchi and the pulmonary arteries and veins could be clearly identified in all the examined species (Figs. 2B, 2E, 2H). No differences in the attenuation of the lung parenchyma after contrast medium injection could be noticed (Table 1). A high prevalence of respiratory diseases, both of bacterial and mycotic origin, is reported in pet parrots[26]. Although neoplastic pathologies are less frequent, a case of pulmonary adenocarcinoma in a blue-and-gold macaw has been reported[27]. It is also possible to find metastatic neoplasia in the lung parenchyma[28]. The use of CT in the diagnosis of respiratory diseases has been widely investigated in snakes[29] but, to the best of the authors' knowledge, no references reporting the CT appearance of respiratory diseases in avian patients are currently available. However, thickened air sacs are a common pathological finding associated with respiratory disease[26-30].

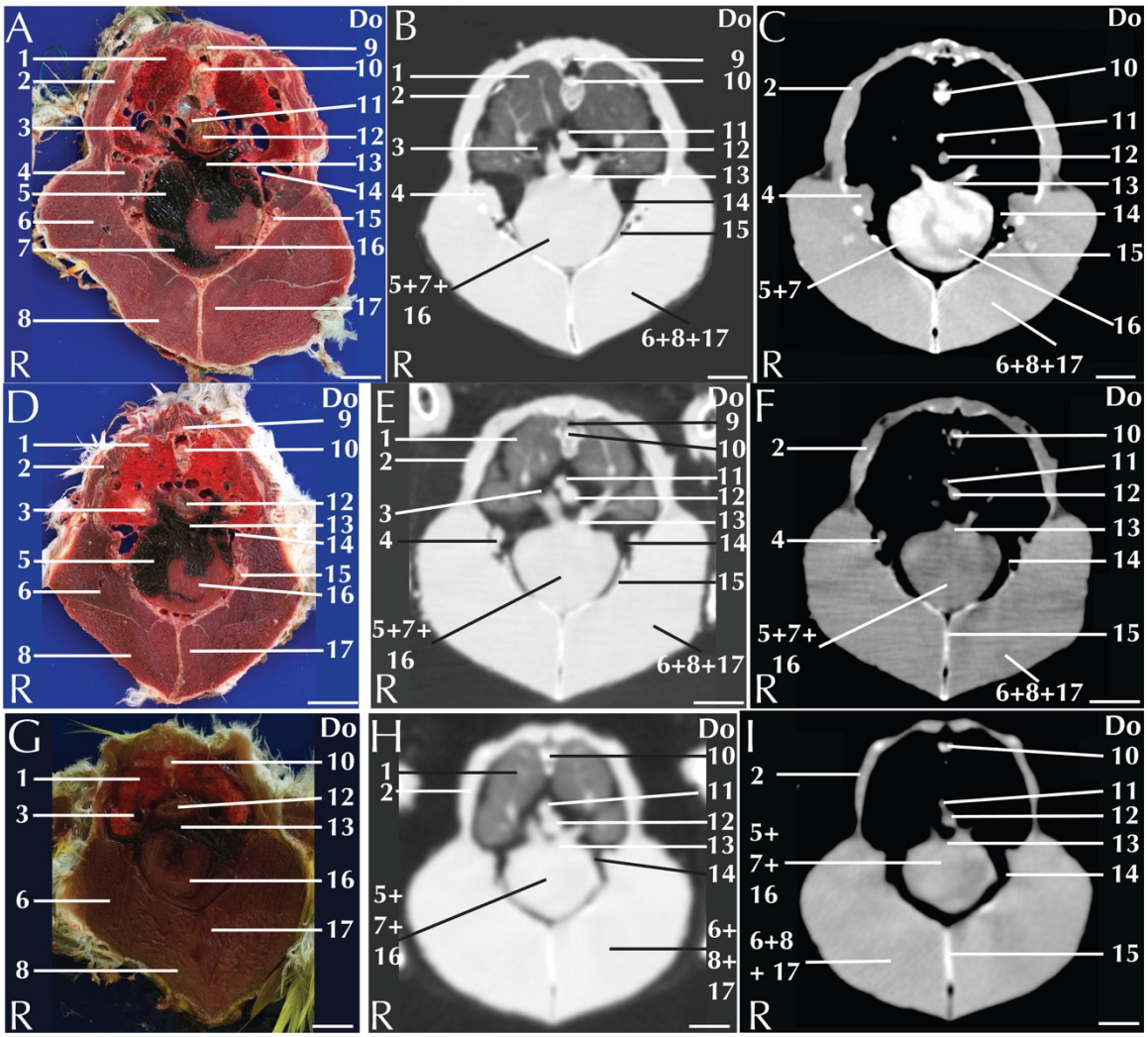

Fig. 2 - Matched cross-sections and CT images at the level of the heart corresponding to line A in Fig. 1. Matched cross-sections and CT images of blue-and-gold macaw (a-c), African grey parrot (d-f) and monk parakeet (g-i). The CT images have been reconstructed with a soft tissue kernel and displayed in pulmonary (b-e-h) and abdomen (c-f-i) window. Do is dorsal and R are right. Bar = 1 cm. 1. Lung; 2. Scapulohumeralis muscle; 3.Intrapulmonary primary bronchus; 4. Scapulohumeral caudal muscle; 5. Right atrium; 6. Pectoral muscle (thoracobrachialis portion); 7. Right ventricle; 8.Pectoral muscle (sternobrachialis portion); 9. Vertebra; 10. Spinal cord; 11. Aorta; 12. Oesophagus; 13. Pulmonary trunk; 14. Cranial thoracic air sac; 15.Carina sterni; 16. Cardiac muscle, left ventricle; 17. Supracoracoid muscle. Do = Dorsal. R = Right. Bar = 1 cm.

The heart is located along the central axis of the body within the coelomic cavity in an indentation of the sternum, cranial to the liver (Figs. 2C, 2F, 2I). The four distinct chambers were visible in the CT images, displayed in an abdominal window in the blue-and-gold macaw (Fig. 2C). The aorta and pulmonary arteries were identified in all the examined species (Figs. 2C, 2F, 2I). It was possible to follow the aorta for its entire length. In birds, the aorta traces a curvy path turning to the right immediately after its ascending portion[31] (Figs. 2C, 2F, 2I).

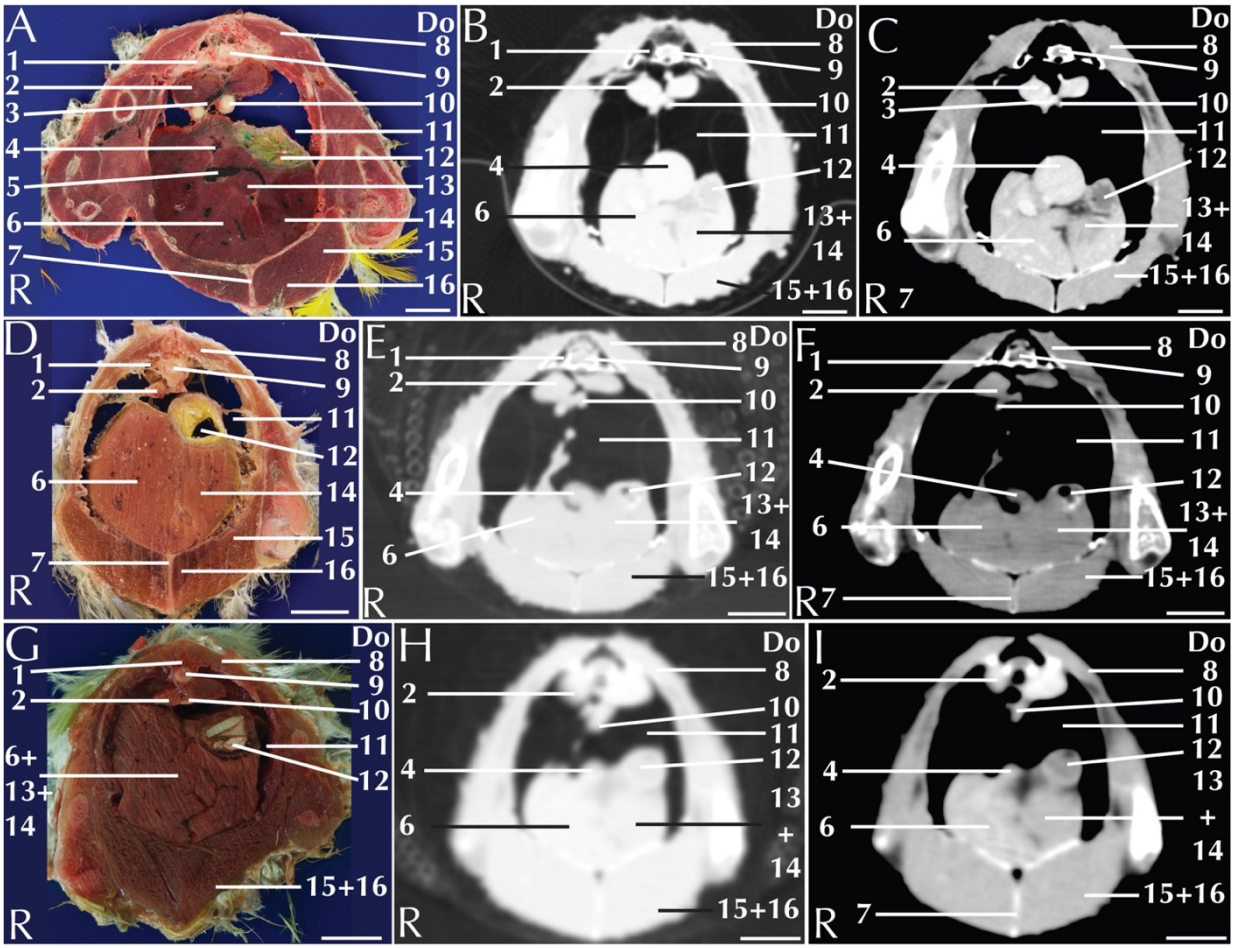

Fig. 3 - Matched cross-sections and CT images at the level of the liver corresponding to line B in Fig. 1. Matched cross-sections and CT images of blue-and-gold macaw (a-c), African grey parrot (d-f) and monk parakeet (g-i). The CT images have been reconstructed with a soft tissue kernel and displayed in pulmonary (b-e-h) and abdomen (c-f-i) window. Do is dorsal and R are right. Bar = 1 cm. 1. Vertebra; 2. Kidney (cranial lobe); 3. Common iliac vein; 4. Spleen; 5. Caudal vena cava; 6. Liver, right lobe; 7. Carina Sterni; 8. Longissimus dorsi muscle; 9. Spinal cord; 10. Gonads; 11. Air sac; 12. Proventriculus; 13. Liver, medial part of the left lobe; 14. Liver, lateral part of the left lobe; 15. Pectoral muscle; 16. Supracoracoid muscle. Do = Dorsal. R = Right. Bar = 1 cm.

The avian liver is a bi-lobed structure that lies on the sternum, wrapping cranially around the heart and dorsally around the lateral margin of the proventriculus. The right lobe is generally bigger than the left in parrots[32] (Figs. 3C, 3F, 3I). Most parrot species, including all the study species, lack gallbladder[32]. In the contrast-enhanced CT images displayed in an abdominal window, the main lobar veins were well visible within a homogeneous parenchyma (Figs. 3C, 3F, 3I, 4C, 4F, 4I). Pre- and post-contrast densities of the liver are reported in Table 1. The liver is a common target for metabolic lipidosis and for bacterial and viral disorders that affect the entire parenchyma or cause disseminated focal necrosis[30].

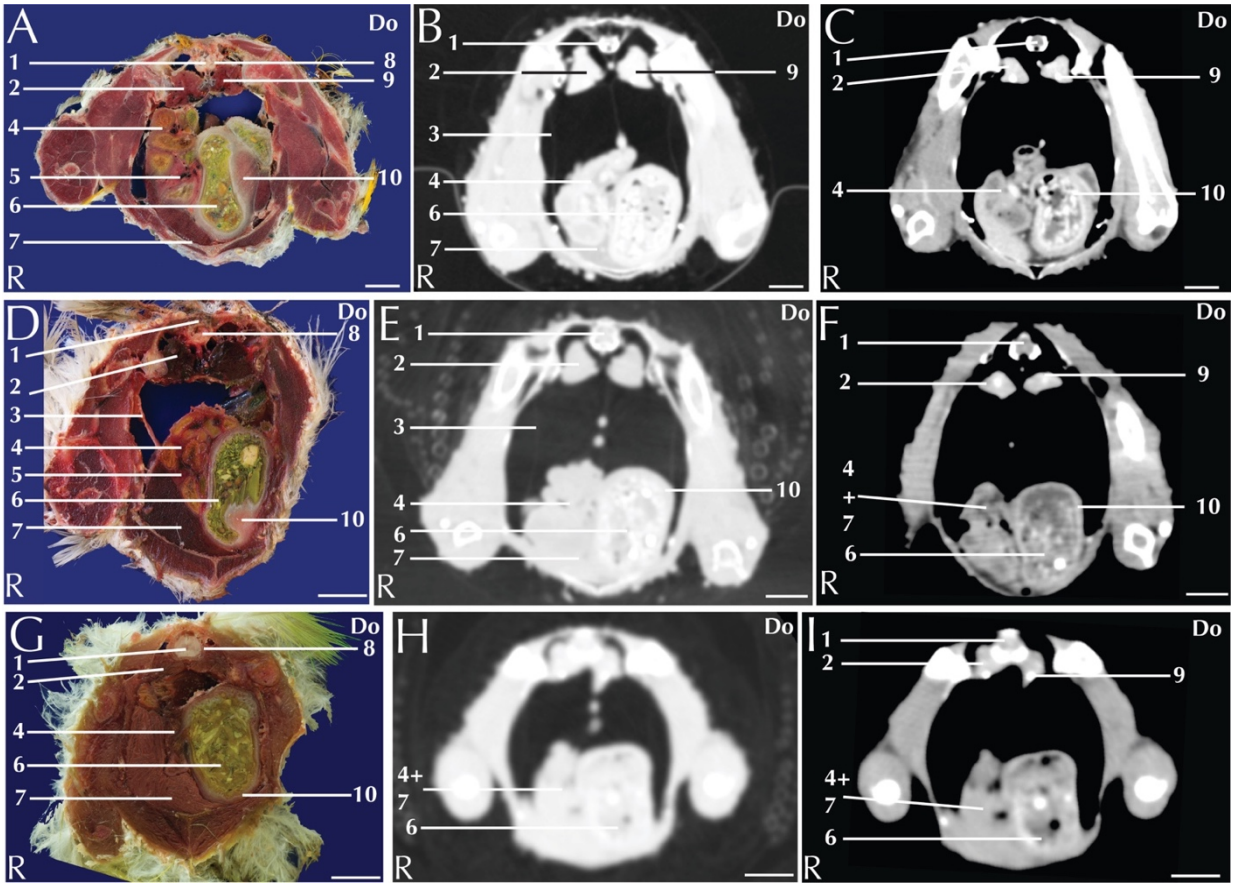

Fig. 4 - Matched cross-sections and CT images at the level of the ventriculus corresponding to line C in Fig. 1. Matched cross-sections and CT images of blue-and-gold macaw (a-c), African grey parrot (d-f) and monk parakeet (g-i). The CT images have been reconstructed with a soft tissue kernel and displayed in pulmonary (b-e-h) and abdomen (c-f-i) window. Do is dorsal and R are right. Bar = 1 cm. 1. Spinal cord; 2. Medial lobe of the right kidney; 3. Air sac wall; 4. Small intestine; 5. Pancreas. 6. Ingesta; 7. Liver; 8. Vertebra; 9. Left ureter; 10. Ventriculus, muscular wall. Do = Dorsal. R = Right. Bar = 1 cm.

The avian stomach is composed of the proventriculus, a glandular portion located after the junction with the oesophagus and the ventriculus, a muscular portion located caudally in the digestive system[33]. The junction between the proventriculus and the ventriculus is called the isthmus. The proventriculus and the ventriculus are clearly visible in the left portion of the coelomic cavity (Figs. 3C, 3F, 3I, 4C, 4F, 4I). The ventriculus has a thick muscular layer that was clearly visible in all the examined species (Figs. 4C, 4F, 4I). In all the study subjects the ventriculus was filled with ingesta that appeared as a mixture of air and dense material with an ill-defined shape (Figs. 4C, 4F, 4I). It was possible to distinguish the grit as a highly attenuating element. Alteration of the stomach, specifically of the proventriculus, can be caused by infective pathologies. In particular, proventricular dilatation disease[34] and Machrorabdus ornitogaster infection could be considered as the most common infection related to alteration of the proventriculus shape. The isthmus is a common localization of Machrorabdus ornitogaster infection and gastric carcinoma[30].

Individual intestinal loops were visible only in the blue-and-gold macaw (Fig. 5C). Intestinal loop attenuation was difficult to evaluate both because of the presence of a mixture of ingesta and air and due to the limited dimensions of the intestinal wall. Nevertheless, the intestines appeared more attenuating in post-contrast scans (Table 1). Intestinal impaction, volvulus and intussusception have been described in avian patients[33]; although mycobacterial lesion (granulomas) can be relatively often recovered in the gut[35] there were no pathologies in our specimens.

The pancreas was located between the descending and ascending duodenal loops and was clearly visible in the anatomical section of blue-and-gold macaw and African grey parrot (4A, 4D), but was not clearly distinguishable in the CT of any of the considered species.

The spleen was visible as a round structure lying to the left of the ventriculus (Figs. 3B, 3E, 3H, 3C, 3F, 3I). Pre- and post-contrast attenuation values of the spleen are reported in Table

1. Several infectious pathologies lead to increased overall dimensions of the spleen[30], but no reference have been made available to date.

Paired kidneys are located lateral to the spine and ventral to the pelvis. Although not clearly distinguishable in transversal CT images, multiplanar reconstructions (not shown in present paper) enabled to individually identify the three distinct lobes of the kidneys (Figs. 5C, 5F, 5I).

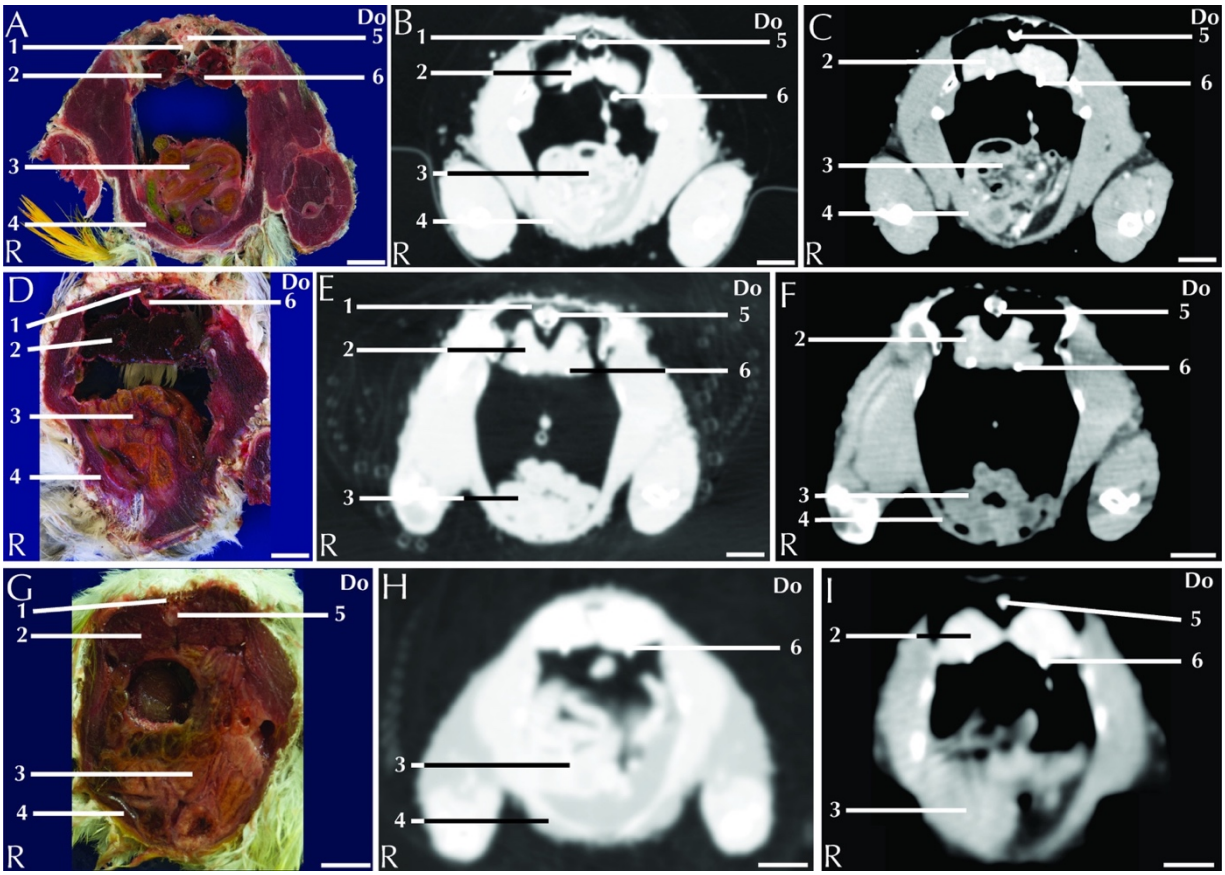

Fig. 5 - Matched cross-sections and CT images at the level of the kidneys corresponding to line D in Fig. 1. Matched cross-sections and CT images of blue-and-gold macaw (a-c), African grey parrot (d-f) and monk parakeet (g-i). The CT images have been reconstructed with a soft tissue kernel and displayed in pulmonary (b-e-h) and abdomen (c-f-i) window. Do is dorsal and R are right. Bar = 1 cm. 1. Vertebra; 2. Medial lobe of the right kidney; 3. Intestine; 4. Pectoral muscle (thoracic portion); 5. Spinal cord; 6. Left ureter. Do = Dorsal. R = Right. Bar = 1 cm.

A corticomedullary distinction was not evident. The ureters were visible, after contrast medium injection, in all the examined species and could be followed from the caudal pole of the kidney to the inlet in the cloaca (Figs. 6B, 6C, 6E, 6F, 6I).

Pre- and post-contrast HU values are reported in Table 1. Renal pathologies are very common in avian patients; changes in shape and size of the renal parenchyma are associated with infections (acute or chronic), or chronic degenerative pathologies[30]. A case of renal tubule neoplasia has been reported in a channel-billed Toucan[36].

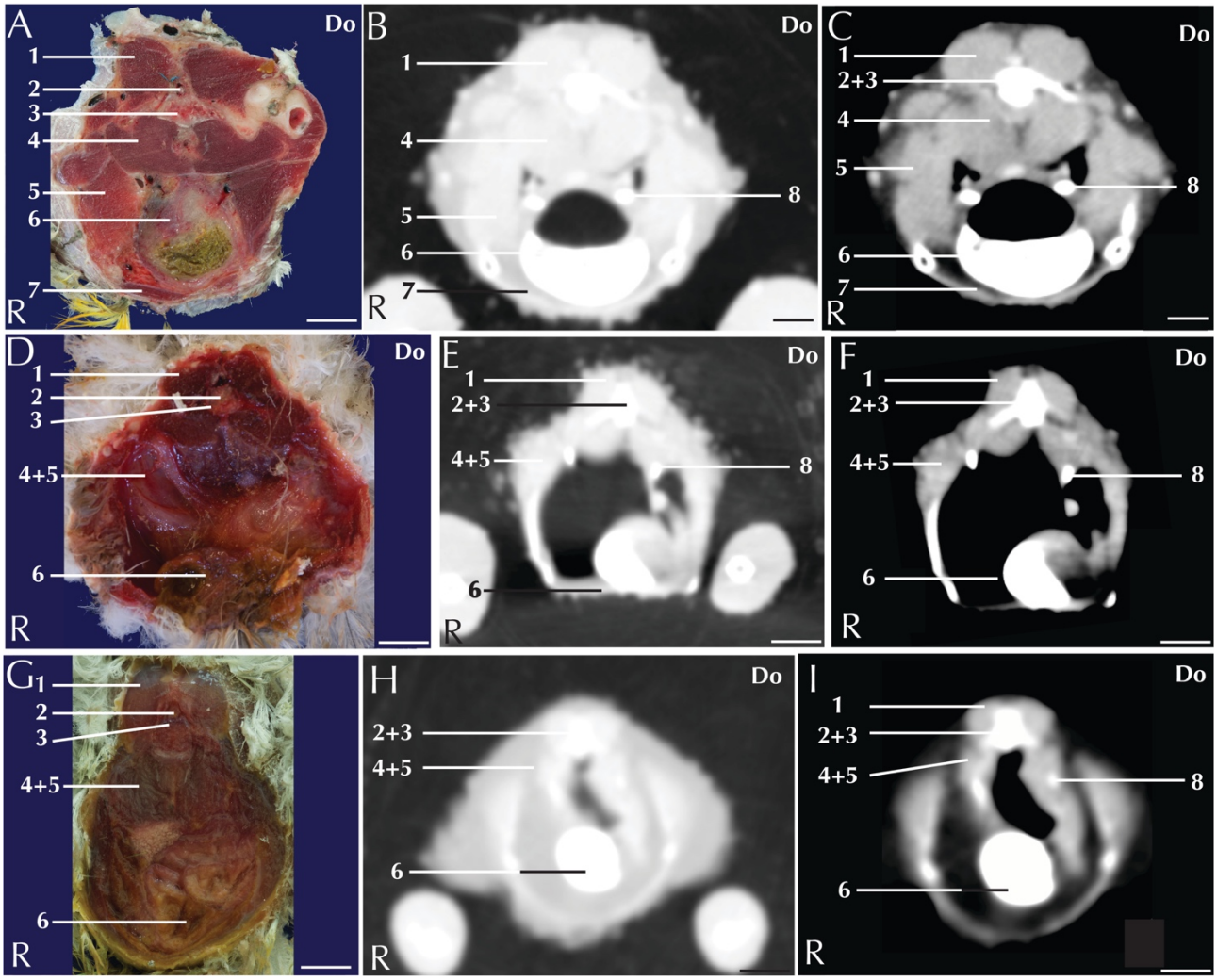

Fig. 6 Matched cross-sections and CT images at the level of the cloaca corresponding to line E in Fig. 1. Matched cross-sections and CT images of blue-and-gold macaw (a-c), African grey parrot (d-f) and monk paraket (g-i). The CT images have been reconstructed with a soft tissue kernel and displayed in pulmonary (b-e-h) and abdomen (c-f-i) window. Do is dorsal and R are right. Bar = 1 cm. 1. Musculus levator caudae; 2. Spinal cord; 3. Vertebra; 4. Musculus levator cloacae; 5. Musculus transversus cloacae; 6. Cloaca; 7. Pectoral muscle (abdominal portion); 8. Left ureter. Do = Dorsal. R = Right. Bar = 1 cm.

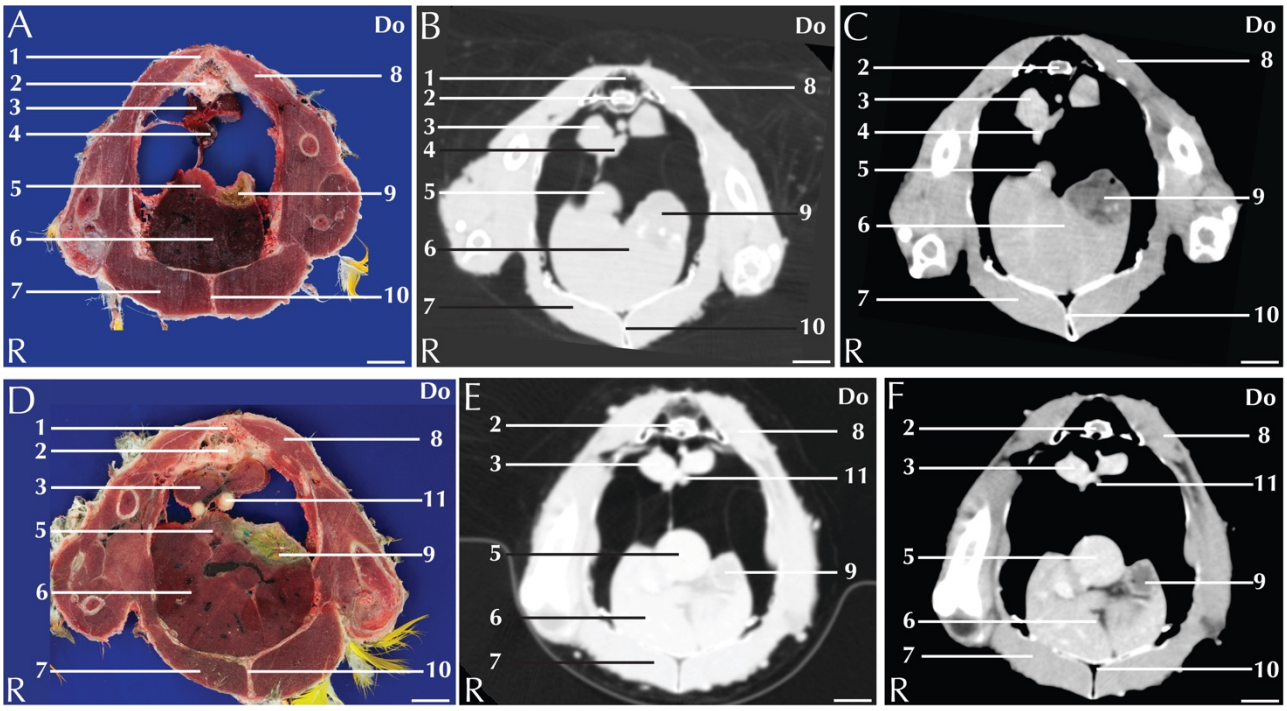

Fig. 7 - Matched cross-sections and CT images at the level of the gonads corresponding to line E in Fig. 1. Matched cross-sections and CT images of female blue-and-gold macaw (a-c), and male blue-and-gold macaw (d-f). The CT images have been reconstructed with a soft tissue kernel and
displayed in pulmonary (b-e) and abdomen (c-f) window. Do is dorsal and R are right. Bar = 1 cm. 1. Vertebra; 2. Spinal cord; 3. Kidney; 4. Ovary; 5. Spleen; 6. Liver; 7. Pectoral muscle; 8. Longissimus dorsi muscle; 9. Proventriculus; 10. Coracoid bone; 11. Testicles. Do = Dorsal. R = Right. Bar = 1 cm.

The gonads are located ventral to the cranial lobe of the kidney (Figs. 7C, 7F). When visible, the testicles appeared as moderately enhancing rounded paired structures whereas the ovaries appeared as single small, slightly elongated structures. In all the considered species, only the left ovary is functional. The gonads were clearly distinguishable only in sexually mature animals of the largest species (5 African grey parrots and 4 blue-and-gold macaw) (Figs. 7C, 7F). Although the gonads were clearly visible, the sex of the animal could not be determined in the smallest species (monk parakeet) because both the ovaries and the testicles had the same CT appearance. The oviduct was not visible in the anatomical images or CT scans. Pre- and post-contrast HU values are reported in Table 1.

Table 1 -. Attenuation values measured in the CT scans of some selected coelomic organs, calculated in pre- and post-contrast CT scans. Pooled data from the considered species are reported.

	Pre-contrast HU values	**Post-contrast HU values**
LIVER [a]	57.20 (33.14- 104.66)	122.99 (86.85 – 172.83)
VENTRICULUS [a]	64.78(36.19 - 91)	116.43 (92.37 – 143.13)
KIDNEY [a]	34.92 (12.39 – 74.86)	178.44 (151.52 – 378.97)
SPLEEN [a]	54.55 (23.11 – 81.3)	141.70 (123.90 – 181.95)
INTESTINE [a]	28.73 (10.8 – 59.53)	77.16 (32.92 – 102.09)
LUNG [a]	-589.47 (-677.26 - -478.48)	-579.97 (-690.50 - -385.73)
AIR SACS [a]	-957.84 (-969 - -929.32)	-982.06 (-1021 - -947.63)
TESTICLE [a]	22.20 (16.93 – 25.31)	47.60 (38.85 – 63.95)
OVARY [a]	15.94 (11.86 – 20.73)	80.97 (65.2 – 91.51)

The reproductive organs of birds undergo cyclic atrophy and enlargement during the year in sexually mature animals[37]. Indeed, the male animals (2 african grey parrots, 1 monk parakeet) scanned during the reproductive season had remarkably larger testicles than the animals (2 blue-and-gold macaws, 1 African grey parrot, 2 monk parakeets) scanned during the non-reproductive period. Testicular and ovarian neoplasia are reported in avian patients[38-39].

Although limited, the use of ultrasonography has been described in birds. The limited dimensions of the coupling sites and the presence of feathers act as limiting factors in the development of this imaging technique in avian patients. Some pathologic conditions, such as fluid accumulation, organ enlargement or displacement of the air sacs, enlarge the coupling site and therefore improve image quality. Ultrasonography is reported to be a

useful diagnostic tool in the differentiation between cardiomegaly and hydropericardium in the investigation of masses involving the female reproductive tract and in the assessment of liver parenchymal changes. Gender determination through ultrasonography is possible only in mature animals during the breeding season; during the rest of the year and in immature animals the visibility of the gonads is hindered by the interposition of air sacs[40].

The lack of superimpositions and the fine anatomical resolution make CT the diagnostic imaging technique of choice when a pathology involving a coelomic organ is suspected. However, the clinician should also bear in mind both the potential risks associated with the general anaesthesia and the possible diagnostic information retrieved from a CT scan.

Conclusions

The matched anatomical cross-sections and CT images presented in this study are a useful reference for the interpretation of CT examination of the blue-and-gold macaw, African grey parrot and monk parakeet.

All the images and descriptions presented in this paper relate only to the above-mentioned species. This atlas can be used as reference for other psittaccine species only if the clinician is aware of the anatomical and physiological differences occurring between the species under investigation and the species considered in this paper.

The complex anatomy of the coelomic cavity and the lack of intracoelomatic fat make the interpretation of plain radiographs often challenging in avian patients; on the other hand, the fine anatomical detail and the scope to evaluate coelomic organ vascularization make CT the gold standard diagnostic imaging modality if a pathology involving the coelomic cavity is suspected.

List of abbreviations

CT: computed tomographic

Ethics approval and consent to participate

* This study was carried out under the approval of the ethics committee (OPBA): Protocol No. 116052; April 28, 2015.

References

1. Groskin R: Prologue. In: Ritchie BW, Harrison GJ, Harrison LR, editors. Avian medicine: principle and application, 1st Ed. Lake Worth, Florida, USA: Wingers publishing inc; 1994. p. 17-25

2. Raftery A. The initial presentation: triage and critical care. In: Harcourt-Brown N, Chitty J, editors. BSAVA Manual of Psittacine Birds, 2nd Ed. Quedgeley, Gloucester, England; British small animal veterinary association; 2005. p. 35-49

3. Alonso-Farré JM, Gonzalo-Orden M, Barreiro-Vázquez JD, Ajenjio JM, Barreiro-Lois A, Llarena-Reino M, et al. Cross-sectional anatomy, computed tomography and magnetic resonance imaging of the thoracic region of common dolphin (*Delphinus delphis*) and striped dolphin (*Stenella coeruleoalba*). Anat Histol Embryol 2014; 43(3): 221-229

4. Endo H, Sasaki H, Hayashi Y, Petrov EA, Amano M, Suzuki N, et al. CT examination of the head of the Baikal seal (*Phoca sibirica*). J Anat 1999; 194(1): 119-126

5. Zotti A, Banzato T, Cozzi B. Cross-sectional anatomy of the rabbit neck and trunk: Comparison of computed tomography and cadaver anatomy. Res Vet Sci 2009; 87(2): 171-176

6. de Rycke LM, Boone MN, Van Caelenberg AI, Dierick M, Van Hoorebeke L, van Bree H, et al. Micro-computed tomography of the head and dentition in cadavers of clinically normal rabbits. Am J Vet Res 2012; 73(2): 227-232

7. Banzato T, Bellini L, Contiero B, Martin A, Balikçi S, Zotti A. Abdominal anatomic features and reference values determined by use of ultrasonography in healthy common rats (*Rattus norvegicus*). Am J Vet Res 2014; 75(1): 67-76

8. Banzato T, Bellini L, Contiero B, Selleri P, Zotti A. Abdominal ultrasound features and reference values in 21 healthy rabbits. Vet Rec 2015; 176(4): 176-101

9. Schumacher J, Toal RL. Advanced radiography and ultrasonography in reptiles. Semin avian exot pet 2001; 10(4): 162-168

10. Arencibia A, Rivero MA, De Miguel I, Contreras S, Cabrero A, Oro S. Computed tomographic anatomy of the head of the loggerhead sea turtle (*Caretta caretta*). Res Vet Sci 2006; 81(2): 65–169

11. Putterill JF, Soley JT. Morphology of the Gular Valve of the Nile Crocodile, Crocodylus niloticus. J Morphol 2006; 267(8): 924-939

12. Banzato T, Russo E, Toma A, Palmisano G, Zotti A. Evaluation of radiographic, computed tomographic, and cadaveric anatomy of the head of boa constrictors. Am J Vet Res 2011; 72(12): 1592-1599

13. Banzato T, Russo E, Finotti L, Zotti A. Development of a technique for contrast radiographic examination of the gastrointestinal tract in ball pythons (*Python regius*). Am J Vet Res 2012; 73(7): 996-1001

14. Banzato T, Selleri P, Veladiano IA, Martin A, Zanetti E, Zotti A. Comparative evaluation of the cadaveric, radiographic and computed tomographic anatomy of the heads

of green iguana (*Iguana iguana*), common tegu (*Tupinambis merianae*) and bearded dragon (*Pogona vitticeps*). BMC Vet Res 2012; 8: 53

15. Banzato T, Selleri P, Veladiano IA, Zotti A. Comparative evaluation of the cadaveric and computed tomographic features of the coelomic cavity in the green iguana (*Iguana iguana*), black and white tegu (*Tupinambis merianae*) and bearded dragon (*Pogona vitticeps*). Anat Histol Embriol 2013; 42(6): 453-460

16. Orosz SE, Toal R. Tomographic anatomy of the golden eagle (*Aquila chrysaetos*). J Zoo Wildl Med 1992; 23(1): 39-46

17. Krautwald-Junghanns ME, Kostka V, Dorsch B. Comparative studies on the diagnostic value of conventional radiography and computed tomography in evaluating the heads of psittacine and raptorial birds. Avian Med Surg 1998;12(3): 149-157

18. Krautwald-Junghanns ME, Valerius K, Duncker H, Sohn HG. CT-assisted versus silicone rubber cast morphometry of the lower respiratory tract in healthy amazons (*Genus amazona*) and grey parrots (*Genus psittacus*). Res Vet Sci 1998; 65(1): 17-22

19. Pepperberg IM, Howell KS, Banta PA, Patterson DK, Meisser M. Measurement of grey parrot (*Psittacus erithacus*) trachea via magnetic resonance imaging, dissection, and electron beam computed tomography. J Morphol 1998; 238(1): 81-91

20. Gumpenberger M, Kolm G. Ultrasonographic and computed tomographic examinations of the avian eye: physiologic appearance, pathologic findings, and comparative biometric measurement. Vet Radiol Ultrasound 2006; 47(5): 492-502

21. Gumpenberger M. Avian. In: Tobias S, Saunders JH, editors. Veterinary computed tomography, 1st Ed. Chichester, West Sussex, England: Wiley-Blackwell; 2011. P. 571-532

22. Krautwald-Junghanns ME, Schroff S, Bartels T. Radiographic investigations. In: Krautwald- Junghanns ME, Pees M, Reese S, Tully T, editors. Diagnostic Imaging of Exotic Pets: Birds, Small Mammals, Reptiles. Hannover, Germany: Schluetersche Verlagsgesellschaft mbH & Co KG; 2011. p. 2-35

23. McLelland J. A colour atlas of avian anatomy. Aylesbury, England: Wolfe Publishing; 1990. p. 1-127

24. Baumel JJ, King AS, Breazile JE, Evans HE, Vanden Berge JC, editors. Handbook of avian anatomy: Nomina Anatomica Avium, 2nd Ed. Cambridge, England: Nuttall Ornithological Club; 1993. p. 1-591

25. Canova M, Clavenzani P, Bombardi C, Mazzoni M, Bedoni C, Grandis A. Anatomy of the shoulder and arm musculature of the common buzzard (*Buteo buteo* Linnaeus, 1758) and the European honey buzzard (*Pernis apivorus* Linnaeus, 1758). Zoomorphol 2015; 134:291-308

26. Thully TN Jr, Harrison GJ. Pneumology. In: Ritchie BW, Harrison GJ, Harrison LR, editors. Avian medicine: principle and application, 1st Ed. Lake Worth, Florida, USA: Wingers publishing inc; 1994. p. 556-581

27. Fredholm DV, Carpenter JW, Schumecher LL, Moon RS. Pulmonary adenocarcinoma with osseous metastasis and secondary paresis in a blue-and-gold macaw (*Ara ararauna*). J Zoo Wildl Med 2012; 43(4): 909-1013

28. Lamb S, Reavill D, Wojcieszyn J, Sitinas N. Osteosarcoma of the tibiotarsus with possible pulmonary metastasis in a ring-necked dove (*Streptopelia risoria*). J Avian Med Surg 2014; 28(1): 50-56.

29. Pees M, Kiefer I, Oechtering G, Krautwald-Junghanns ME. Computed tomography for the diagnosis and treatment monitoring of bacterial pneumonia in Indian pythons (*Python molurus*). Vet Rec 2008; 163(5): 152-156

30. Dorrestein GM, de Wit M. Clinical pathology and necropsy In: Harcourt-Brown N, Chitty J, editors. BSAVA Manual of Psittacine Birds, 2nd Ed. Quedgeley, Gloucester, England: British small animal veterinary association; 2005. p. 60-86

31. Lumeij JT, Branson WR. Cardiology. In: Ritchie BW, Harrison GJ, Harrison LR, editors. Avian medicine: principle and application, 1st Ed. Lake Worth, Florida, USA: Wingers publishing inc; 1994. p. 695-722

32. Lumeij JT. Hepatology. In: Ritchie BW, Harrison GJ, Harrison LR, editors. Avian medicine: principle and application, 1st Ed. Lake Worth, Florida, USA: Wingers publishing inc; 1994. p. 522-537

33. Lumeij JT. Gastroenterology. In: Ritchie BW, Harrison GJ, Harrison LR, editors, Avian medicine: principle and application, 1st Ed. Lake Worth, Florida, USA: Wingers publishing inc; 1994. p. 482–521

34. Staeheli P, Rinder M, Kaspers B. Avian bornavirus associated with fatal disease in psittacine birds. J Virol 2010; 84(13): 6269-6275

35. Panigrahy B, Clark FD, Hall CF. Mycobacteriosis in psittacine birds. Avian Dis 1983; 27(4): 1166-1168

36. Mainez M, Cardona T, Such R, Juan-Sallés C, Garner MM. Bilateral Renal Tubular Neoplasm in a Channel-billed Toucan (*Ramphastos vitellinus*). J Avian Med Surg 2015; 29(1): 46-50

37. Taylor M. Endoscopic examination and biopsy techniques. In: Ritchie BW, Harrison GJ, Harrison LR, editors. Avian medicine: principle and application, 1st Ed. Lake Worth, Florida, USA: Wingers publishing inc; 1994. p. 343

38. Campbell TW. Citology. In: Ritchie BW, Harrison GJ, Harrison LR, editors. Avian medicine: principles and application, 1st Ed. Lake Worth, Florida, USA:Wingers publishing inc; 1994. p. 199-222

39. Uetsuka K, Suzuki T, Doi K, Nunoya T. Malignant sertoli cell tumor in a goose (*Anser cygnoides domesticus*). Avian Dis 2012; 56(4): 781-785

40. Krautwald-Junghanns ME, Pees M. Ultrasonographic examination. In: Krautwald-Junghanns ME, Pees M, Reese S, Tully T, editors. Diagnostic Imaging of Exotic Pets: Birds,

Small Mammals, Reptiles. Hannover, Germany: Schluetersche Verlagsgesellschaft mbH & Co KG; 2011. p. 36-136

General discussion

The evolution of the avian medicine and the increasing use of the CT scan with those patients has highlighted the need of a complete and easy-to-consult atlas of the normal tomographic appearance of birds.

During this research the tomographic images of blue and gold macaw, African gray parrot and monk parakeet were analyzed and compared with the corresponding anatomic slices.

The complex anatomy of the avian head and coelomic cavity makes the interpretation of the radiographies really challenging. The computed tomography allows the clinician to have high detailed images of all the anatomic districts without the problem of the superimpositons.
One of the best result was achieved in the visualization of the respiratory system, including the head's pneumatized bones, the air sacs, the pulmonary bronchial system and the lungs parenchima.
The possibility to analyze those districts avoiding the superimpositions increases the probability to detect a pathological process, leading to a best and faster treatment.

The size of the animal remains one of the main limiting factor. Nevertheless it is possible to obtain images with diagnostic significance of animals of 120-130 grams. Moreover, the possibility to inject the intravenous contrast even in those small patients further increase the quality of the exam.

The anesthesia for the CT scan is usually a safe procedure, both because the very short time request for this exam and the noninvasive nature of this exam.

The result of this work confirmed the value of the tomographic examination as a quick and reliable diagnostic tool.

Ringraziamenti

Arrivata al termine di questa avventura voglio ringraziare di cuore tutti coloro che mi hanno aiutata e sostenuta.

Il mio capo, il professor Zotti, che ha creduto in me e mi ha supportata durante questi tre anni, nonostante le notevoli difficoltà incontrate durante il percorso.

Tommaso, che nonostante i numerosi impegni ha sempre trovato il tempo di aiutarmi. Senza di lui sicuramente il dottorato sarebbe stato molto diverso.

Luca, insostituibile anestesista che in questi tre anni ha superato le sue perplessità nei confronti delle più svariate creature. Non penso lo ammetterà mai, ma sospetto che comincino a piacergli.

Alessia, che nonostante la sua avversione per i volatili mi ha sempre incoraggiata e aiutata, sotto ogni punto di vista.

Federico, Andrea, Magdalena, Laura, Lisa, Michele, Helen, Matteo, Beatrice, Melissa, Clarissa, Luca, Francesco, Graziano, Lillo, Paolo che in questi tre anni hanno reso speciale ogni giorno.

Paolo, Tommaso, Alessandro, Alessandra, Ivano e tutti gli altri colleghi e amici del CVS di Roma. Grazie per avermi aiutata in questa ricerca ma soprattutto grazie per la meravigliosa esperienza che è stata lavorare con voi.

Salvatore, Federica, Barbara e tutti i veterinari della sezione di patologia aviare dell' IzsVenezie, per avermi aiutata per questi articoli e per avermi insegnato tanto.

Un grazie special ai miei genitori, che ancora una volta mi sono stati vicini e hanno sempre creduto in me, nonostante le bizzarrie del mio lavoro. Senza il loro aiuto nulla di tutto questo sarebbe stato possibile.

Un enorme ringraziamento a tutto il resto della mia famiglia, che ormai si è rassegnata a vedermi poco.

Grazie a Chiara, Silvia, Laura, Jessica, Serena, Marta che ci sono sempre state, anche se purtroppo ci si vede poco.

Grazie ad Alberto, Emilio, Luca, Francesca, Lorenzo, Gaia, Michele, Kasia insostituibili compagni di numerose serate.

E, ultimo ma non ultimo, un gigantesco grazie a Enrico, che mi è stato vicino, ha sopportato me e le mie gatte ed è sopravvissuto ai racconti delle mie giornate lavorative.